

TECHNICAL REPORT



**Metallic communication cable test methods –
Part 4-1: Electromagnetic compatibility (EMC) – Introduction to electromagnetic
(EMC) screening measurements**

WithNorm.com: Click to view the full PDF of IEC TR 62153-4-1:2010



THIS PUBLICATION IS COPYRIGHT PROTECTED

Copyright © 2010 IEC, Geneva, Switzerland

All rights reserved. Unless otherwise specified, no part of this publication may be reproduced or utilized in any form or by any means, electronic or mechanical, including photocopying and microfilm, without permission in writing from either IEC or IEC's member National Committee in the country of the requester.

If you have any questions about IEC copyright or have an enquiry about obtaining additional rights to this publication, please contact the address below or your local IEC member National Committee for further information.

Droits de reproduction réservés. Sauf indication contraire, aucune partie de cette publication ne peut être reproduite ni utilisée sous quelque forme que ce soit et par aucun procédé, électronique ou mécanique, y compris la photocopie et les microfilms, sans l'accord écrit de la CEI ou du Comité national de la CEI du pays du demandeur.

Si vous avez des questions sur le copyright de la CEI ou si vous désirez obtenir des droits supplémentaires sur cette publication, utilisez les coordonnées ci-après ou contactez le Comité national de la CEI de votre pays de résidence.

IEC Central Office
3, rue de Varembe
CH-1211 Geneva 20
Switzerland
Email: inmail@iec.ch
Web: www.iec.ch

About IEC publications

The technical content of IEC publications is kept under constant review by the IEC. Please make sure that you have the latest edition, a corrigenda or an amendment might have been published.

- Catalogue of IEC publications: www.iec.ch/searchpub

The IEC on-line Catalogue enables you to search by a variety of criteria (reference number, text, technical committee,...). It also gives information on projects, withdrawn and replaced publications.

- IEC Just Published: www.iec.ch/online_news/justpub

Stay up to date on all new IEC publications. Just Published details twice a month all new publications released. Available on-line and also by email.

- Electropedia: www.electropedia.org

The world's leading online dictionary of electronic and electrical terms containing more than 20 000 terms and definitions in English and French, with equivalent terms in additional languages. Also known as the International Electrotechnical Vocabulary online.

- Customer Service Centre: www.iec.ch/webstore/custserv

If you wish to give us your feedback on this publication or need further assistance, please visit the Customer Service Centre FAQ or contact us:

Email: csc@iec.ch
Tel.: +41 22 919 02 11
Fax: +41 22 919 03 00

TECHNICAL REPORT



**Metallic communication cable test methods –
Part 4-1: Electromagnetic compatibility (EMC) – Introduction to electromagnetic
(EMC) screening measurements**

INTERNATIONAL
ELECTROTECHNICAL
COMMISSION

PRICE CODE **XB**

ICS 33.100, 33.120.10

ISBN 978-2-88910-918-0

CONTENTS

FOREWORD.....	5
1 Scope.....	7
2 Normative references.....	7
3 Electromagnetic phenomena.....	8
4 The intrinsic screening parameters of short cables.....	10
4.1 General.....	10
4.2 Surface transfer impedance, Z_T	10
4.3 Capacitive coupling admittance, Y_C	10
4.4 Injecting with arbitrary cross-sections.....	12
4.5 Reciprocity and symmetry.....	12
4.6 Arbitrary load conditions.....	12
5 Long cables – coupled transmission lines.....	12
6 Transfer impedance of a braided wire outer conductor or screen.....	20
7 Test possibilities.....	26
7.1 General.....	26
7.2 Measuring the transfer impedance of coaxial cables.....	26
7.3 Measuring the transfer impedance of cable assemblies.....	26
7.4 Measuring the transfer impedance of connectors.....	27
7.5 Calculated maximum screening level.....	27
8 Comparison of the frequency response of different triaxial test set-ups to measure the transfer impedance of cable screens.....	32
8.1 General.....	32
8.2 Physical basics.....	32
8.2.1 Triaxial set-up.....	32
8.2.2 Coupling equations.....	35
8.3 Simulations.....	35
8.3.1 General.....	35
8.3.2 Simulation of the standard and simplified methods according to EN 50289-1-6, IEC 61196-1 (method 1 and 2) and IEC 62153-4-3 (method A).....	36
8.3.3 Simulation of the double short circuited methods.....	43
8.4 Conclusion.....	51
9 Background of the shielded screening attenuation test method (IEC 62153-4-4).....	52
9.1 General.....	52
9.2 Objectives.....	52
9.3 Theory of the triaxial measuring method.....	53
9.4 Screening attenuation.....	58
9.5 Normalised screening attenuation.....	59
9.6 Measured results.....	60
9.7 Comparison with absorbing clamp method.....	62
9.8 Practical design of the test set-up.....	63
9.9 Influence of mismatches.....	64
Annex A (normative) List of symbols.....	67
Bibliography.....	70
Figure 1 – Total electromagnetic field (\vec{E}_t, \vec{H}_t).....	8

Figure 2 – Defining and measuring screening parameters – A triaxial set-up	9
Figure 3 – Equivalent circuit for the testing of Z_T	11
Figure 4 – Equivalent circuit for the testing of $Y_c = j \omega C_T$	11
Figure 5 – Electrical quantities in a set-up that is matched at both ends	12
Figure 6 – The summing function $S\{L \cdot f\}$ for near and far end coupling	16
Figure 7 – Transfer impedance of a typical single braid screen	17
Figure 8 – The effect of the summing function-coupling transfer function of a typical single braid screen cable	17
Figure 9 – Calculated coupling transfer functions T_n and T_f for a single braid – $Z_F = 0$	18
Figure 10 – Calculated coupling transfer functions T_n and T_f for a single braid – $\text{Im}(Z_T)$ is positive and $Z_F = +0,5 \times \text{Im}(Z_T)$ at high frequencies	18
Figure 11 – Calculated coupling transfer functions T_n and T_f for a single braid – $\text{Im}(Z_T)$ is negative and $Z_F = -0,5 \times \text{Im}(Z_T)$ at high frequencies	19
Figure 12 – $L \cdot S$: the complete length dependent factor in the coupling function T	20
Figure 13 – Transfer impedance of typical cables	21
Figure 14 – Magnetic coupling in the braid Complete flux	22
Figure 15 – Magnetic coupling in the braid Left-hand lay contribution	22
Figure 16 – Magnetic coupling in the braid Right-hand lay contribution	22
Figure 17 – Complex plane, $Z_T = \text{Re } Z_T + j \text{Im } Z_T$, frequency f as parameter	23
Figure 18 – Magnitude (amplitude), $ Z_T(f) $	23
Figure 19 – Typical Z_T (time) step response of an overbraided and underbraided single braided outer conductor of a coaxial cable	24
Figure 20 – Z_T equivalent circuits of a braided wire screen	25
Figure 21 – Comparison of signal levels in a generic test setup	28
Figure 22 – Triaxial set-up for the measurement of the transfer impedance Z_T	32
Figure 23 – Equivalent circuit of the triaxial set-up	33
Figure 24 – Simulation of the frequency response for g	37
Figure 25 – Simulation of the frequency response for g	37
Figure 26 – Simulation of the frequency response for g	38
Figure 27 – Simulation of the frequency response for g	38
Figure 28 – Simulation of the 3 dB cut off wavelength (L/λ_1)	39
Figure 29 – Interpolation of the simulated 3 dB cut off wavelength (L/λ_1)	40
Figure 30 – 3 dB cut-off frequency length product as a function of the dielectric permittivity of the inner circuit (cable)	41
Figure 31 – Measurement result of the normalised voltage drop of a single braid screen in the triaxial set-up	42
Figure 32 – Measurement result of the normalised voltage drop of a single braid screen in the triaxial set-up	43
Figure 33 – Triaxial set-up (measuring tube), double short circuited method	44
Figure 34 – Simulation of the frequency response for g	45
Figure 35 – Simulation of the frequency response for g	45
Figure 36 – Simulation of the frequency response for g	46
Figure 37 – Simulation of the frequency response for g	46
Figure 38 – Interpolation of the simulated 3 dB cut off wavelength (L/λ_1)	47

Figure 39 – 3 dB cut-off frequency length product as a function of the dielectric permittivity of the inner circuit (cable)	48
Figure 40 – Simulation of the frequency response for g	49
Figure 41 – Interpolation of the simulated 3 dB cut off wavelength (L/λ_1).....	50
Figure 42 – 3 dB cut-off frequency length product as a function of the dielectric permittivity of the inner circuit (cable)	50
Figure 43 – Definition of transfer impedance.....	52
Figure 44 – Definition of coupling admittance	52
Figure 45 – Triaxial measuring set-up for screening attenuation.....	53
Figure 46 – Equivalent circuit of the triaxial measuring set-up	54
Figure 47 – Calculated voltage ratio for a typical braided cable screen.....	55
Figure 48 – Calculated periodic functions for $\epsilon_{r1} = 2,3$ and $\epsilon_{r2} = 1,1$	56
Figure 49 – Calculated voltage ratio-typical braided cable screen.....	57
Figure 50 – Equivalent circuit for an electrical short part of the length Δl and negligible capacitive coupling.....	58
Figure 51 – a_s of single braid screen, cable type RG 58, $L = 2$ m.....	61
Figure 52 – a_s of single braid screen, cable type RG 58, $L = 0,5$ m.....	61
Figure 53 – a_s of cable type HF 75 0,7/4,8 02YCY.....	62
Figure 54 – a_s of cable type HF 75 1,0/4,8 02YCY.....	62
Figure 55 – a_s of double braid screen, cable type RG 223.....	62
Figure 56 – Schematic for the measurement of the screening attenuation a_s	64
Figure 57 – Short circuit between tube and cable screen of the CUT	64
Figure 58 – Triaxial set-up, impedance mismatches.....	65
Figure 59 – Calculated voltage ratio including multiple reflections caused by the screening case.....	66
Figure 60 – Calculated voltage ratio including multiple reflections caused by the screening case.....	66
Table 1 – The coupling transfer function T (coupling function).....	15
Table 2 – Screening effectiveness of cable test methods for surface transfer impedance Z_T ..	30
Table 3 – Load conditions of the different set-ups.....	34
Table 4 – Parameters of the different set-ups	36
Table 5 – Cut-off frequency length product	40
Table 6 – Typical values for the factor v , for an inner tube diameter of 40 mm and a generator output impedance of 50 Ω	44
Table 7 – Cut-off frequency length product	47
Table 8 – Material combinations and the factor n	49
Table 9 – Cut-off frequency length product	50
Table 10 – Cut-off frequency length product for some typical cables in the different set-ups...	51
Table 11 – Δa in dB for typical cable dielectrics	60
Table 12 – Comparison of results of some coaxial cables	63

INTERNATIONAL ELECTROTECHNICAL COMMISSION

METALLIC COMMUNICATION CABLE TEST METHODS –**Part 4-1: Electromagnetic compatibility (EMC) –
Introduction to electromagnetic (EMC) screening measurements**

FOREWORD

- 1) The International Electrotechnical Commission (IEC) is a worldwide organization for standardization comprising all national electrotechnical committees (IEC National Committees). The object of IEC is to promote international co-operation on all questions concerning standardization in the electrical and electronic fields. To this end and in addition to other activities, IEC publishes International Standards, Technical Specifications, Technical Reports, Publicly Available Specifications (PAS) and Guides (hereafter referred to as "IEC Publication(s)"). Their preparation is entrusted to technical committees; any IEC National Committee interested in the subject dealt with may participate in this preparatory work. International, governmental and non-governmental organizations liaising with the IEC also participate in this preparation. IEC collaborates closely with the International Organization for Standardization (ISO) in accordance with conditions determined by agreement between the two organizations.
- 2) The formal decisions or agreements of IEC on technical matters express, as nearly as possible, an international consensus of opinion on the relevant subjects since each technical committee has representation from all interested IEC National Committees.
- 3) IEC Publications have the form of recommendations for international use and are accepted by IEC National Committees in that sense. While all reasonable efforts are made to ensure that the technical content of IEC Publications is accurate, IEC cannot be held responsible for the way in which they are used or for any misinterpretation by any end user.
- 4) In order to promote international uniformity, IEC National Committees undertake to apply IEC Publications transparently to the maximum extent possible in their national and regional publications. Any divergence between any IEC Publication and the corresponding national or regional publication shall be clearly indicated in the latter.
- 5) IEC itself does not provide any attestation of conformity. Independent certification bodies provide conformity assessment services and, in some areas, access to IEC marks of conformity. IEC is not responsible for any services carried out by independent certification bodies.
- 6) All users should ensure that they have the latest edition of this publication.
- 7) No liability shall attach to IEC or its directors, employees, servants or agents including individual experts and members of its technical committees and IEC National Committees for any personal injury, property damage or other damage of any nature whatsoever, whether direct or indirect, or for costs (including legal fees) and expenses arising out of the publication, use of, or reliance upon, this IEC Publication or any other IEC Publications.
- 8) Attention is drawn to the Normative references cited in this publication. Use of the referenced publications is indispensable for the correct application of this publication.
- 9) Attention is drawn to the possibility that some of the elements of this IEC Publication may be the subject of patent rights. IEC shall not be held responsible for identifying any or all such patent rights.

The main task of IEC technical committees is to prepare International Standards. However, a technical committee may propose the publication of a technical report when it has collected data of a different kind from that which is normally published as an International Standard, for example "state of the art".

IEC/TR 62153-4-1, which is a technical report, has been prepared by IEC technical committee 46: Cables, wires, waveguides, R.F. connectors, R.F. and microwave passive components and accessories.

This second edition cancels and replaces the first edition published in 2007. The significant change is a new clause on the background of the shielded screening attenuation test method.

The text of this technical report is based on the following documents:

Enquiry draft	Report on voting
46/331/DTR	46/350/RVC

Full information on the voting for the approval of this technical report can be found in the report on voting indicated in the above table.

This publication has been drafted in accordance with the ISO/IEC Directives, Part 2.

A list of all parts of the IEC 62153 series, under the general title: *Metallic communication cable test methods*, can be found on the IEC website.

The committee has decided that the contents of this publication will remain unchanged until the stability date indicated on the IEC web site under "<http://webstore.iec.ch>" in the data related to the specific publication. At this date, the publication will be

- reconfirmed,
- withdrawn,
- replaced by a revised edition, or
- amended.

A bilingual version of this publication may be issued at a later date.

IMPORTANT – The 'colour inside' logo on the cover page of this publication indicates that it contains colours which are considered to be useful for the correct understanding of its contents. Users should therefore print this document using a colour printer.

METALLIC COMMUNICATION CABLE TEST METHODS –

Part 4-1: Electromagnetic compatibility (EMC) – Introduction to electromagnetic (EMC) screening measurements

1 Scope

Screening (or shielding) is one basic way of achieving electromagnetic compatibility (EMC). However, a confusingly large number of methods and concepts is available to test for the screening quality of cables and related components, and for defining their quality. This technical report gives a brief introduction to basic concepts and terms trying to reveal the common features of apparently different test methods. It should assist in correct interpretation of test data, and in the better understanding of screening (or shielding) and related specifications and standards.

2 Normative references

The following referenced documents are indispensable for the application of this document. For dated references, only the edition cited applies. For undated references, the latest edition of the referenced document (including any amendments) applies.

IEC 60096-1:1986, *Radio-frequency cables – Part 1: General requirements and measuring methods*
Amendment 2 (1993)

IEC 60096-4-1, *Radio-frequency cables – Part 4: Specification for superscreened cables – Section 1: General requirements and test methods*

IEC 60169-1-3, *Radio frequency connectors – Part 1: General requirements and measuring methods – Section 3: Electrical tests and measuring procedures – Screening effectiveness*

IEC 61196-1:1995, *Radiofrequency cables – Part 1: Generic specification – General, definitions, requirements and test methods*

IEC 61726, *Cable assemblies, cables, connectors and passive microwave components – Screening attenuation measurement by the reverberation chamber method*

IEC 62153-4-3, *Metallic communication cables test methods – Part 4-3: Electromagnetic compatibility (EMC) – Surface transfer impedance – Triaxial method*

IEC 62153-4-4, *Metallic communication cable test methods – Part 4-4: Electromagnetic compatibility (EMC) – Shielded screening attenuation, test method for measuring of the screening attenuation a_s up to and above 3 GHz*

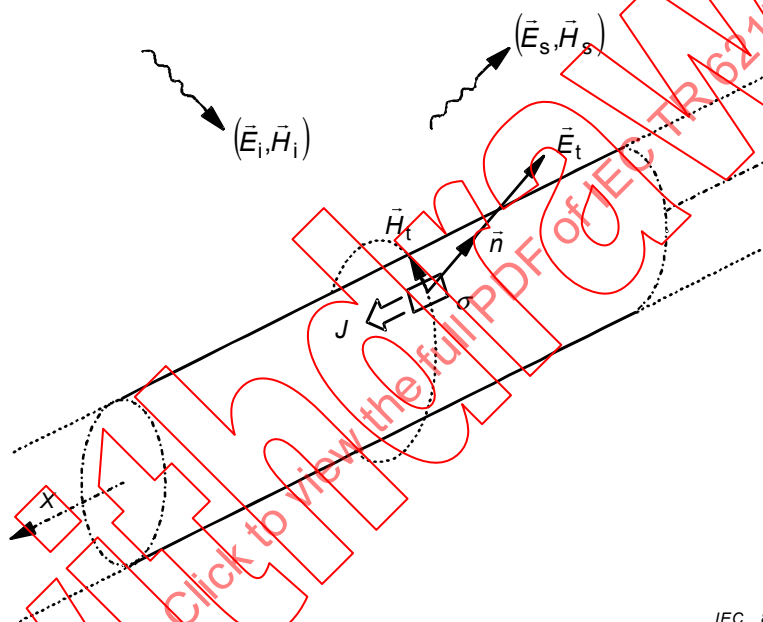
IEC 62153-4-5, *Metallic communication cable test methods – Part 4-5: Electromagnetic compatibility (EMC) – Coupling or screening attenuation – Absorbing clamp method*

EN 50289-1-6, *Communication cables – Specification for test methods – Electrical test methods – Electromagnetic performance*

3 Electromagnetic phenomena

It is assumed that if an electromagnetic field is incident on a screened cable, there is only weak coupling between the external field and that inside, and that the cable diameter is very small compared with both the cable length and the wavelength of the incident field. The superposition of the external incident field and the field scattered by the cable yields the total electromagnetic field (\vec{E}_t, \vec{H}_t) in Figure 1. The total field at the screen's surface may be considered as the source of the coupling: electric field penetrates through apertures by electric or capacitive coupling; also magnetic fields penetrate through apertures by inductive or magnetic coupling.

Additionally, the induced current in the screen results in conductive or resistive coupling.



IEC 893/10

Key

(\vec{E}_i, \vec{H}_i)	incident electromagnetic field	J	induced surface current density- (A/m)
(\vec{E}_s, \vec{H}_s)	scattered electromagnetic field	σ	induced surface charge density- (C/m ²)
(\vec{E}_t, \vec{H}_t)	total electromagnetic field	\vec{n}	unit vector normal to the surface
x	positive axial cable direction	ϵ_0, ϵ_r	permittivity, free space and relative

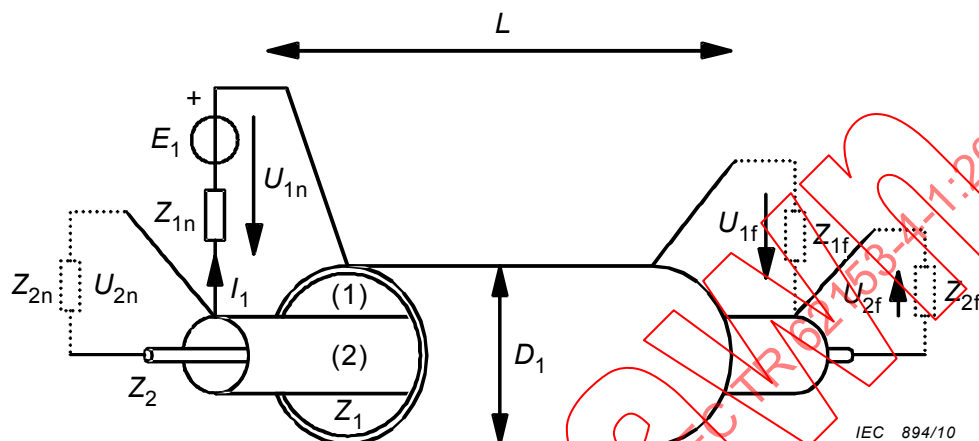
Figure 1 – Total electromagnetic field (\vec{E}_t, \vec{H}_t)

$$(\vec{E}_t, \vec{H}_t) = (\vec{E}_i, \vec{H}_i) + (\vec{E}_s, \vec{H}_s) \quad (1)$$

$$J = \vec{n} \cdot \vec{H}_t \quad (2)$$

$$\sigma = \vec{n} \cdot \vec{E}_t \epsilon_0 \epsilon_r \quad (3)$$

As the field at the surface of the screen is directly related to density of surface current and surface charge, the coupling may be assigned either to the total field (\vec{E}_t, \vec{H}_t) or to the surface current- and charge- densities (J and σ). Consequently, the coupling into the cable may be simulated by reproducing, through any suitable means, the surface currents and charges on the screen. Because the cable diameter is assumed to be small, the higher modes may be neglected and it is possible to use an additional coaxial conductor as the injection structure, as shown in Figure 2.



Key (for Figures 2,3,4,5)

- (1), (2) Indicates outer circuit(1), tube, respectively inner circuit(2), cable
- $Z_{1,2}$ Characteristic impedance of the outer circuit(1), tube, respectively inner circuit(2), cable
- $\epsilon_{1,2}$ Dielectric permittivity of the outer circuit(1), tube, respectively inner circuit(2), cable
- $\beta_{1,2}$ Phase constant of the outer circuit(1), tube, respectively inner circuit(2), cable
- $\lambda_{1,2}$ Wave length of the outer circuit(1), tube, respectively inner circuit(2), cable
- L Coupling length
- D_1 Diameter of injection cylinder-tube
- V Voltmeter
- A Ammeter
- Z_{1n}, Z_{1f} Load resistance at the near end, respectively far end of the outer circuit(1), tube
- Z_{2n}, Z_{2f} Load resistance at the near end, respectively far end of the inner circuit(2), cable
- E_1 EMF of the generator
- I_1, I_2 Current in the outer circuit(1), tube, respectively inner circuit(2), cable
- U_{1n}, U_{1f} Voltage at the near end, respectively far end of the outer circuit(1), tube
- U_{2n}, U_{2f} Voltage at the near end, respectively far end of the inner circuit(2), cable
- Concept of a triaxial set-up
- (1) outer circuit (1), formed by an injection cylinder-tube and the screen under test, with characteristic impedance Z_1 ,
- (2) inner circuit (2), formed by the screen under test, and centre conductor, with characteristic impedance Z_2 ; screening at the ends of circuit (2) is not shown.

Observe the conditions Z_{1f}, Z_{2n}, Z_{2f} and λ in Figure 3 and Figure 4.

NOTE 1 $D_1 \ll L$.

NOTE 2 Both ends of circuit (2) must be well screened.

Figure 2 – Defining and measuring screening parameters – A triaxial set-up

4 The intrinsic screening parameters of short cables

4.1 General

The intrinsic parameters refer to an infinitesimal length of cable, like the inductance or capacitance per unit length of transmission lines. Assuming electrically short cables, with $L \ll \lambda$ which will always apply at low frequencies, the intrinsic screening parameters are defined and can be measured as indicated in the following subclauses.

4.2 Surface transfer impedance, Z_T

As shown in Figure 3, where Z_{1f} and Z_{2f} are zero, the surface transfer impedance (Z_T in Ω/m) is given:

$$Z_T = \frac{U_{2n}}{I_1 \cdot L} \quad (4)$$

The dependence of Z_T on frequency is not simple and is often shown by plotting $\log Z_T$ against \log frequency. Note that the phase of Z_T may have any value, depending on braid construction and frequency range.

NOTE In circuit (2) of Figure 3, the voltmeter and short circuit can be interchanged.

4.3 Capacitive coupling admittance, Y_C

As shown in Figure 4, where Z_{1f} and Z_{2f} are open circuit, the capacitive coupling admittance (Y_C in mho/m) is given by:

$$Y_C = j \cdot \omega \cdot C_T = \frac{I_2}{U_{1n} \cdot L} \quad (5)$$

where

C_T is the through capacitance;

ω is the radian frequency;

j is the imaginary operator.

The through capacitance C_T is a real capacitance and has usually a constant value up to 1 GHz and higher (with aperture $a \ll \lambda$).

While Z_T is independent of the characteristics of the coaxial circuits (1) and (2), C_T is dependent on those characteristics. There are two ways of overcoming this dependence:

- a) The normalized through elastance K_T (with units of m/F) derived from C_T is independent of the size of the outer coaxial circuit (2), but it depends on its permittivity:

$$K_T = C_T / (C_1 \cdot C_2) \quad (6)$$

$$K_T \sim 1/(\epsilon_{r1} + \epsilon_{r2}) \quad (7)$$

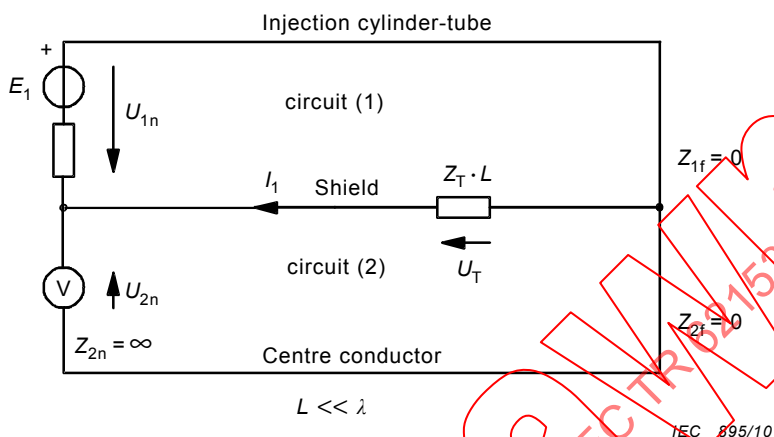
where C_1 and C_2 are the capacitance per unit length of the two coaxial circuits.

- b) The capacitive coupling impedance Z_F (with units of Ω/m) again derived from C_T is also independent of the size of the outer coaxial circuit (2) and, for practical values of ϵ_{r1} , is only slightly dependent on its permittivity:

$$Z_F = Z_1 Z_2 Y_C = Z_1 Z_2 j \omega C_T \quad (8)$$

$$Z_F \sim \sqrt{(\epsilon_{r1} \cdot \epsilon_{r2})} / (\epsilon_{r1} + \epsilon_{r2}) \quad (9)$$

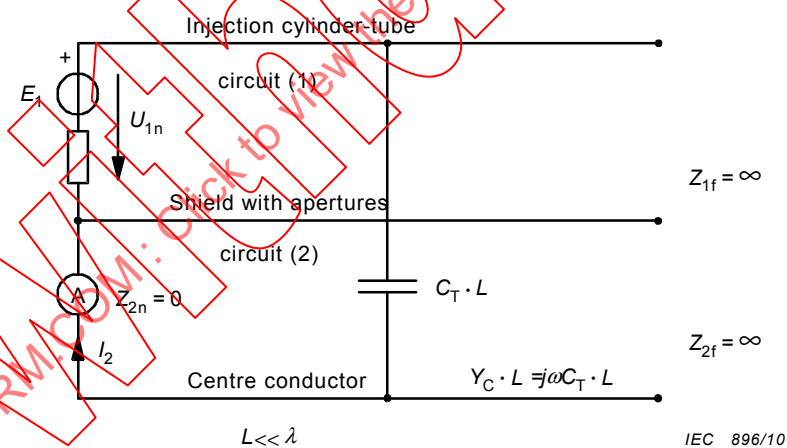
Compared with Z_T , Z_F is usually negligible, except for open weave braids. It may, however, be significant when Z_{2n} and $Z_{2f} \gg Z_2$ (audio circuits).



Key

See Figure 2.

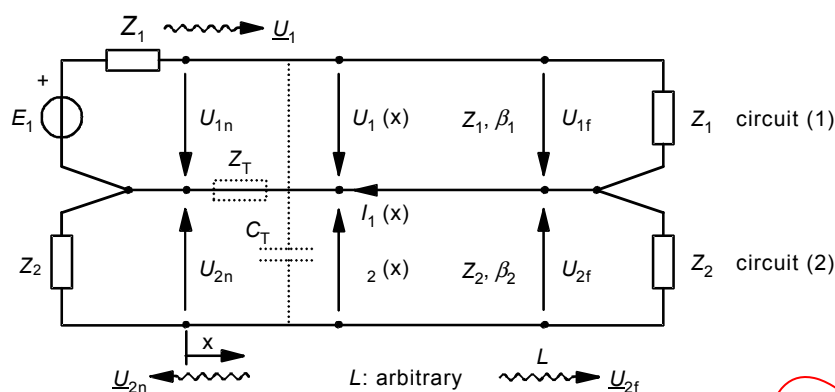
Figure 3 – Equivalent circuit for the testing of Z_T



Key

See Figure 2.

Figure 4 – Equivalent circuit for the testing of $Y_C = j \omega C_T$



Key

See Figure 2.

NOTE Z_T and C_T are distributed (not correctly shown here). The loads Z_1 , Z_2 at the ends may represent matched receivers.

Figure 5 – Electrical quantities in a set-up that is matched at both ends

4.4 Injecting with arbitrary cross-sections

A coaxial outer circuit (2) has been assumed so far in this report, but it is not essential because of the invariance of Z_T and Z_F . Using a wire in place of the outer cylinder, the injection circuit (2) becomes two-wire with the return via the screen of the cable under test. Obviously the charge and current distribution become non-uniform, but the results are equivalent to coaxial injection, especially if two injection lines are used opposite to each other, and may be justified for worst-case testing. Note that the IEC line injection test uses a wire.

4.5 Reciprocity and symmetry

Assuming linear shield materials, the measured Z_T and Z_F values will not change when interchanging the injection circuit (1) and the measuring circuit (2). Each of the two conductors of the two-line circuit can be interchanged, but in practice the set-up will have to take into account possible ground loops and coupling to the environment.

4.6 Arbitrary load conditions

When the circuit ends of Figure 3 and Figure 4 are not ideally a short or open circuit, Z_T and Z_F will act simultaneously. Their superposition is noticeable in the low frequency coupling of the matched circuit (1) and circuit (2), (Figure 5 and Table 1).

5 Long cables – coupled transmission lines

The coupling over the whole length of the cable is obtained by summing up (integrating) the infinitesimal coupling contributions along the cable while observing the correct phase. The analysis utilizes the following assumptions and conventions:

- matched circuits considered with the voltage waves \underline{U}_1 , \underline{U}_{2n} , \underline{U}_{2f} , see Figure 5,
- representation of the coupling, using the normalized wave amplitudes $\underline{U}/\sqrt{Z} [\sqrt{\text{Watt}}]$, instead of voltage waves. i.e. the coupling transfer function, in the following denoted by "coupling function", will be defined as

$$T_n = \frac{\underline{U}_{2n} / \sqrt{Z_2}}{\underline{U}_1 / \sqrt{Z_1}} \quad (10)$$

$$T_f = \frac{U_{2f} / \sqrt{Z_2}}{U_1 / \sqrt{Z_1}} \quad (11)$$

NOTE 1 $|T|^2$ is the ratio of the power waves travelling in circuits (2) and (1). Due to reciprocity and assuming linear screen (shield) materials, T is reciprocal, i.e. invariant with respect to the interchange of injection and measuring circuits (1) and (2).

NOTE 2 The quantity $|1/T|^2$, or in logarithmic quantities

$$a_s = -20 \times \log_{10} |T| \quad (12)$$

may be considered as the "screening attenuation" of the cable, specific to the set-up.

Performing the straight forward calculations of coupled transmission line theory, the coupling function T , given in Table 1, is obtained. The term $S\{L \cdot f\}$ is the "summing function" S , being dependent on L and f . (The wavy bracket just indicates that the product $L \cdot f$ is the argument of the function S and not a factor to S). S represents the phase effect, when summing up the infinitesimal couplings along the line, and is:

$$S_n \{L \cdot f\} = \frac{\sin \frac{\beta L \pm}{2}}{\frac{\beta L \pm}{2}} \exp \left(-j \cdot \frac{\beta L \pm}{2} \right) \quad (13)$$

with

$$\beta L \pm = (\beta_2 \pm \beta_1) \cdot L \quad (14)$$

$$= 2\pi L f \cdot (1/v_2 \pm 1/v_1) \quad (15)$$

$$= 2\pi L f \cdot (\sqrt{\epsilon_{r2}} \pm \sqrt{\epsilon_{r1}}) / c \quad (16)$$

subscript \pm refers to near/far end respectively;
 $+$ refers to both near/far ends.

Note that weak coupling, i.e. $T \ll 1$, has been assumed. This case, including losses, is given in [1]¹⁾.

Equation (17) and the representation in Table 1 illustrate the contributions of the different parameters to the coupling function T :

$$T_n = (Z_F \pm Z_T) \cdot \frac{1}{\sqrt{Z_1 \cdot Z_2}} \cdot \frac{L}{2} \cdot S_n \{L \cdot f, \epsilon_{r1}, \epsilon_{r2}\} \quad (17)$$

Note especially the following points.

- There may be a directional effect ($T_n \neq T_f$) in the whole frequency range if Z_F is not negligible. (But Z_F is usually negligible except with loose, single braid shields.)
- Up to a constant factor, T is the quantity directly measured in a set-up.

¹⁾ Figures in square brackets refer to the bibliography.

- c) For low frequencies, i.e. for short cables ($L \ll \lambda$), the trivial coupling formula is obtained that is directly proportional to L :

$$T_{nf} = (Z_F \pm Z_T) \cdot \frac{1}{Z_{12}} \cdot \frac{L}{2} \quad (18)$$

where

$$Z_{12} = \sqrt{Z_1 \cdot Z_2}$$

- d) The summing function $S\{L \cdot f\}$ is presented in Figure 6.

- e) $S\{L \cdot f\}$ has a $\sin(x)/x$ behaviour. A cut-off point may be defined as $(L \cdot f)_c$:

$$(L \cdot f)_{cn} = \frac{c}{\pi \left| \sqrt{\epsilon_{r1}} \pm \sqrt{\epsilon_{r2}} \right|} \quad (19)$$

- f) The exact envelope of $S\{L \cdot f\}$ is

$$\text{Env} \left| S_{nf} \{L \cdot f\} \right| = \frac{1}{\sqrt{1 + \frac{(L \cdot f)^2}{(L \cdot f)_{cn}^2}}} \quad (20)$$

Table 1 – The coupling transfer function T (coupling function)^a

Set-up parameters ^b	
$(Z_1), L, \epsilon_{r1}$	
$T_n = (Z_F \pm Z_T) \cdot \frac{1}{\sqrt{Z_1 \cdot Z_2}} \cdot \frac{L}{2} \cdot S_n \{L \cdot f, \epsilon_{r1}, \epsilon_{r2}\}$	
$\sqrt{\quad}$ Intrinsic screen parameters	$\sqrt{\quad}$ Cable parameters ^b $(Z_2, L), \epsilon_{r2}$
$\sqrt{\quad}$ "Low-frequency coupling", short cables ^c	$\sqrt{\quad}$ "HF-effect" cut-off $(L \cdot f)_c$. $\sqrt{\quad}$ Length + frequency effect
^a T^2 is the power coupling from circuit (1) to circuit (2). The stacked subscripts _f ⁿ are associated to the stacked operation symbols \pm in the obvious way: upper subscript \rightarrow upper operation, lower subscript \rightarrow lower operation. ^b ϵ_{r1} and ϵ_{r2} contained in S as parameters. ^c for $L \ll \lambda$: $S\{L \cdot f\} \rightarrow 1$.	

- g) The first minimum (zero) of $S\{L \cdot f\}$ occurs at

$$(L \cdot f)_{\min} = \pi(L \cdot f)_c \quad (21)$$

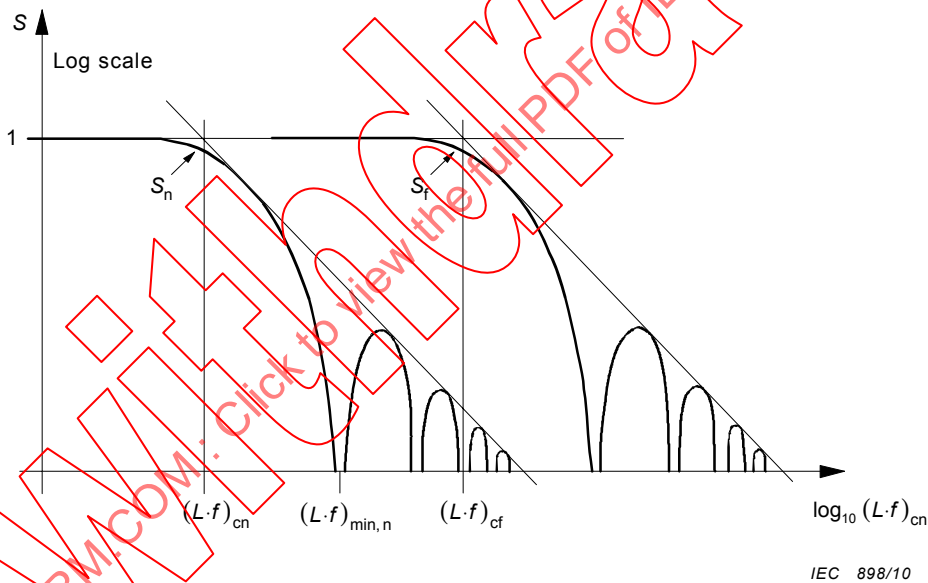
- h) As seen from Equations (13) and (20), below the cut-off points $(L \cdot f)_{cn}$ is $S\{L \cdot f\} \approx 1$ and above them it starts to oscillate and its envelope drops asymptotically 20 dB/decade,

$$\text{Env} \left| S_n \{L \cdot f\} \right|_f \approx \frac{\left(\frac{(L \cdot f)_{cn}}{f} \right)}{(L \cdot f)} \quad (22)$$

- i) S is symmetrical in L and f , i.e. L and f are interchangeable. For a fixed length a cut-off frequency f_c and vice versa, for a fixed frequency a cut-off length L_c may be defined. Substituting c/λ_0 for f , we obtain the cut-off length as

$$L_{cn} = \frac{\lambda_0}{\pi \sqrt{\epsilon_{r1} \pm \sqrt{\epsilon_{r2}}}} \quad (23)$$

- j) The effect of S in the frequency range ($L = \text{constant}$) is illustrated in Figure 8. The coupling function is proportional to Z_T , only if $f < f_c$. Note also the typical values indicated for f_c .
- k) The minima and maxima of S are not resonances, they are due to cancelling and additive effects of the coupling along the line.
- l) The far end cut-off frequency is significantly influenced by the permittivity of the outer system (ϵ_{r1}). Selecting $\epsilon_{r1} \rightarrow \epsilon_{r2}$ we obtain $(L \cdot f)_{cf} \rightarrow \infty$, i.e. no cut-off at the far end. Due to practical aspects (tolerances, homogeneity, etc.), an ideal phase matching ($\epsilon_{r1} \equiv \epsilon_{r2}$) is not feasible.
- m) The effects of Z_T and Z_F on the coupling transfer functions T_n and T_f are shown in Figure 8.
- n) The total effect of L on the coupling is not contained in S alone, but in the product $L \cdot S\{L \cdot f\}$. The product $L \cdot S$ is presented in Figure 12 for $f = \text{constant}$. The coupling function T which can be measured in a set-up, is proportional to L if $L < L_c$. However, for appropriately long cables ($L > L_c$), the maximum coupling is independent of L and we obtain a length independent shielding attenuation above the cut-off point $(L \cdot f)_c$. But we should remember that $(L \cdot f)_c$ as well as A_s are still dependent on the set-up parameters (ϵ_{r1}, Z_1).



NOTE $S_f > S_n$ above near end cut-off, yielding a directive effect.

$(L \cdot f)_c$: cut-off point

Figure 6 – The summing function $S\{L \cdot f\}$ for near and far end coupling

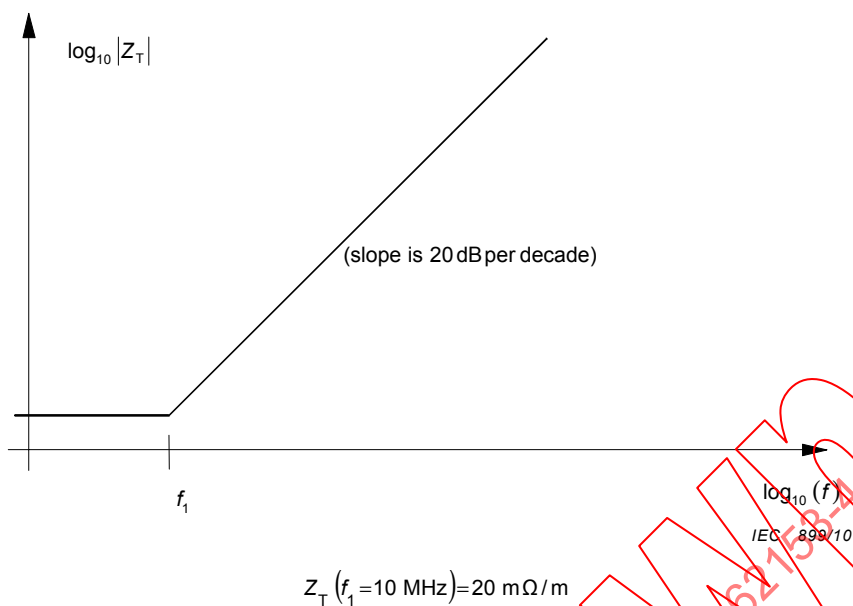
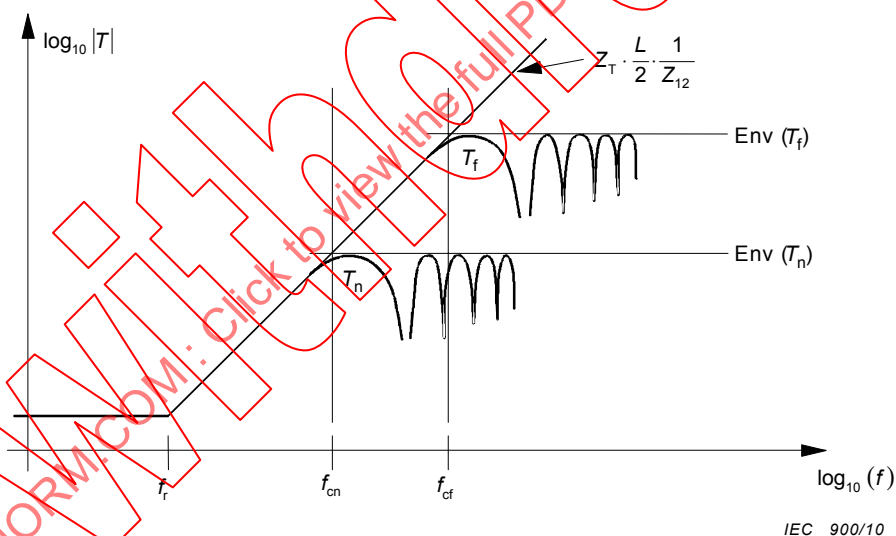


Figure 7 – Transfer impedance of a typical single braid screen

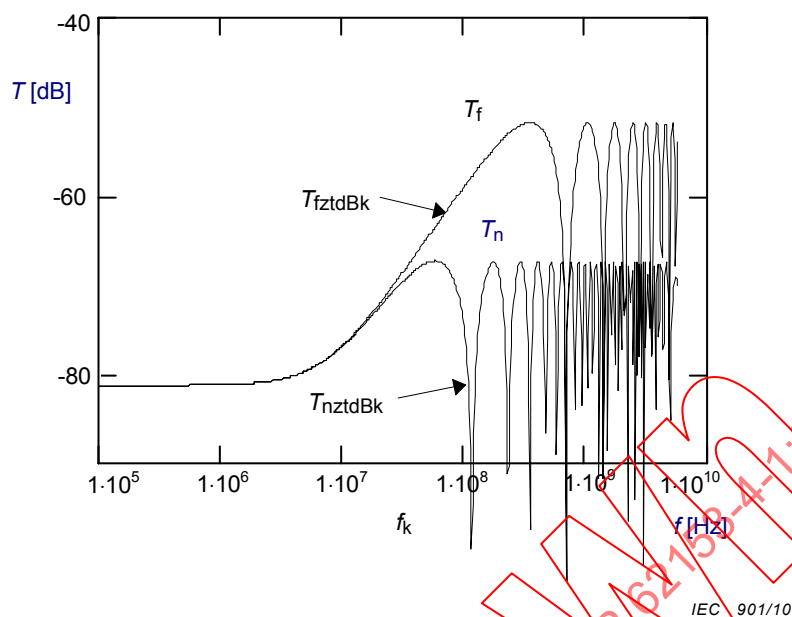
Figure 8 gives the result of adding (on a log scale) the frequency responses from Figure 6 and Figure 7. It is assumed the cable has negligible Z_F ($Z_F \ll Z_T$)



Example: $\epsilon_{r1} = 1$ (set-up), $\epsilon_{r2} = 2.2$ (cable)

$L = 1 \text{ m}$; $f_{cn} = 40 \text{ MHz}$; $f_{cf} = 200 \text{ MHz}$

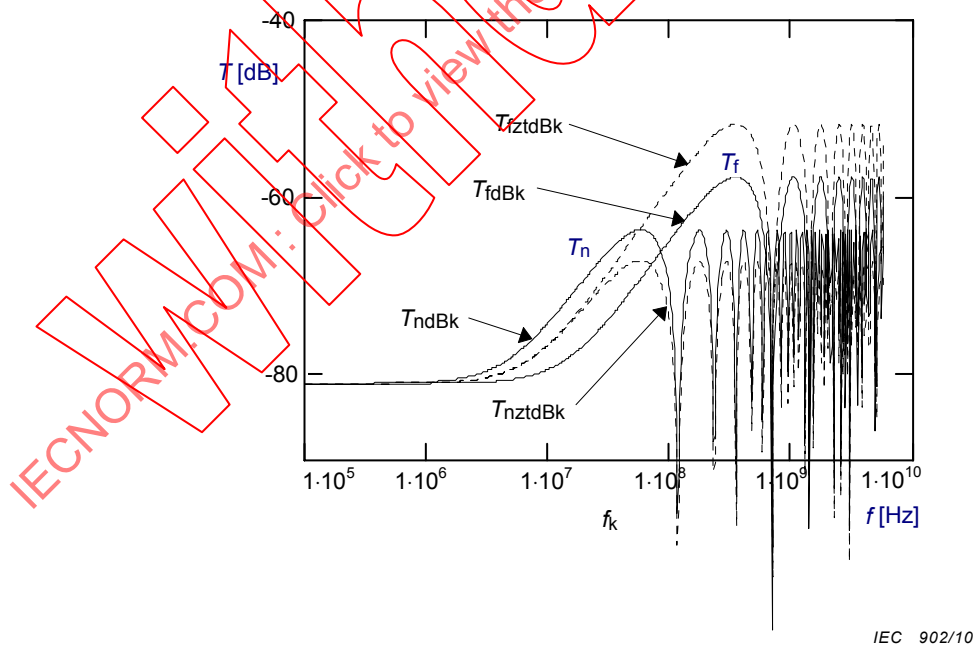
Figure 8 – The effect of the summing function-coupling transfer function of a typical single braid screen cable



In calculations the following parameters are used:

Z_T (d.c.) = 15 mΩ/m and Z_T (10 MHz) = 20 mΩ/m increasing 20 dB/decade (see Figure 7), cable length 1 m, and velocities of the outer and inner line: $v_1 = 200$ Mm/s and $v_2 = 280$ Mm/s corresponding to a velocity difference of 40 %.

Figure 9 – Calculated coupling transfer functions T_n and T_f for a single braid – $Z_F = 0$

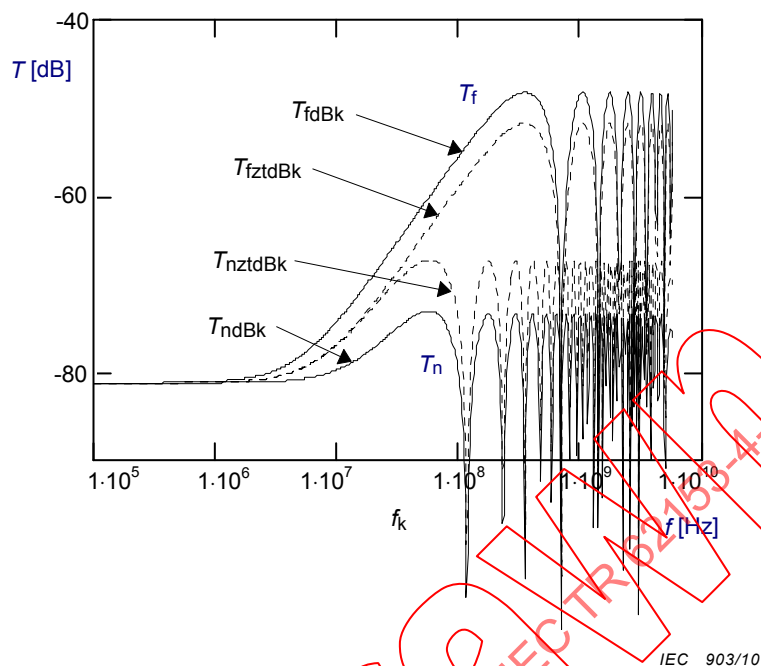


T_n is 3,5 dB higher and T_f is 6 dB lower than in reference Figure 9 because

$$T_n \sim |Z_F + Z_T| = 1,5 \times Z_T \text{ and}$$

$$T_f \sim |Z_F - Z_T| = 0,5 \times Z_T$$

Figure 10 – Calculated coupling transfer functions T_n and T_f for a single braid – $\text{Im}(Z_T)$ is positive and $Z_F = +0,5 \times \text{Im}(Z_T)$ at high frequencies



T_f is 3,5 dB higher and T_n is 6 dB lower than in reference Figure 9 because

$$T_f \sim |Z_F - Z_T| = 1,5 \times |Z_T| \text{ and } T_n \sim |Z_F + Z_T| = 0,5 \times |Z_T|$$

Figure 11 – Calculated coupling transfer functions T_n and T_f for a single braid – $\text{Im}(Z_T)$ is negative and $Z_F = -0,5 \times \text{Im}(Z_T)$ at high frequencies

In Figure 9, $Z_F = 0$ and Z_T is positive.

In Figure 10 and 11, Z_F is significant ($Z_F = (1/2) \times Z_T$).

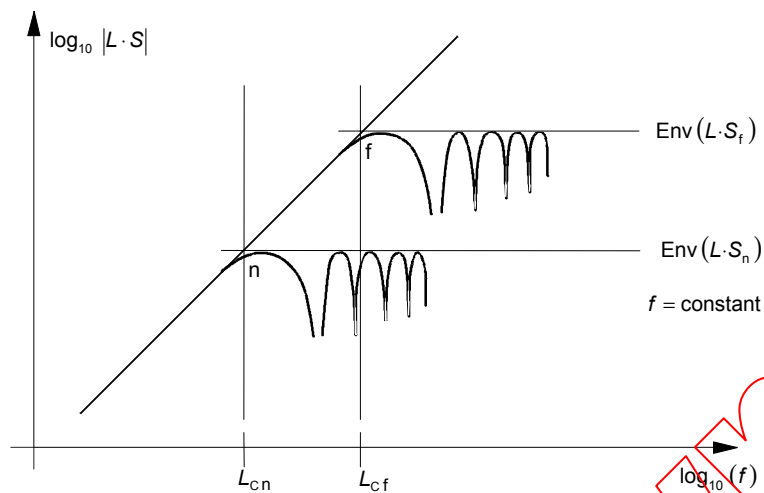
In Figure 11, Z_T is negative at high frequencies.

The following notes apply to Figures 9, 10, and 11.

NOTE 1 T_n for near-end, T_f for far-end and dB means that $T_{n,f}$ are calculated in dB ($20 \times \log_{10} |T_{n,f}|$)

NOTE 2 T_n dB: near-end when $Z_F = (1/2) \times Z_T$ and T_{nzt} dB: near-end when $Z_F = 0$.

NOTE 3 T_f dB: far-end when $Z_F = (1/2) \times Z_T$ and T_{fzt} dB: far-end when $Z_F = 0$.



NOTE 1 For $L > L_c$, the maximum value of T is attained, i.e. the maximum coupling (or the screening attenuation) is not dependent on L .

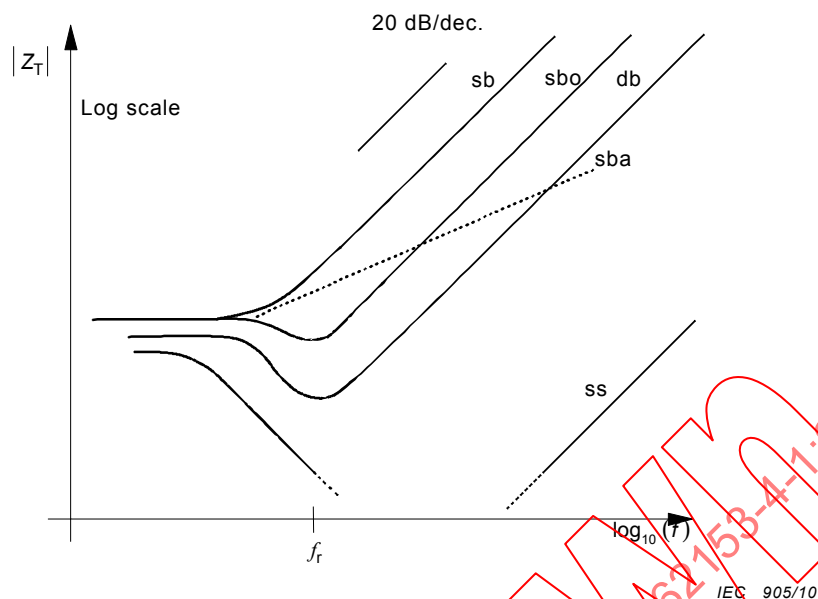
NOTE 2 L_{cf} strongly depends on ϵ_{r1} .

NOTE 3 See also Table 1 and list item n)

Figure 12 – $L \cdot S$: the complete length dependent factor in the coupling function T

6 Transfer impedance of a braided wire outer conductor or screen

Typical transfer impedances of cables with braided wire screens are shown in Figure 13. The constant Z_T value at the low-frequency end is equal to the DC resistance of the screen, the 20 dB per decade rise at the high-frequency end is due to the inductive coupling through the screen and the dip at the middle frequencies is caused by eddy currents or skin effect of the braid. Some braided cables may behave anomalously having less than a 20 dB per decade rise at high frequencies. By using an extrapolation of 20 dB per decade we are in most cases on the conservative side. This extrapolation can be used up to several GHz.



Key

f_r : typically 1....10 MHz

sb: single braid

sbo: single braid optimized

sba: single braid 'anomalous'

db: double braid

ss: superscreen

Figure 13 – Transfer impedance of typical cables

An electrically short piece of braided coaxial cable (2) is considered to be placed in a triaxial arrangement as in Figure 2.

It is assumed that the outer circuit (1) is the disturbing one. As stated a braided cable has a transfer impedance Z_T that increases proportionally to frequency at high frequencies, because of the leakage of the magnetic field through holes in the braid.

The total flux of the magnetic field induced by the disturbing current I_1 is Φ_1 . A part of it, Φ'_{12} leaks directly through the holes and includes a disturbing voltage U'_2 in the inner circuit. However, a part Φ''_{12} of Φ_1 flows in the braid and complicates the mechanism of the total magnetic leakage by the following additional phenomenon:

The braiding wires alternate between the outer and inner layer. It means that the inner and outer braid wires are likewise ingredients of both the inner (2) and outer (1) circuit of Figure 14.

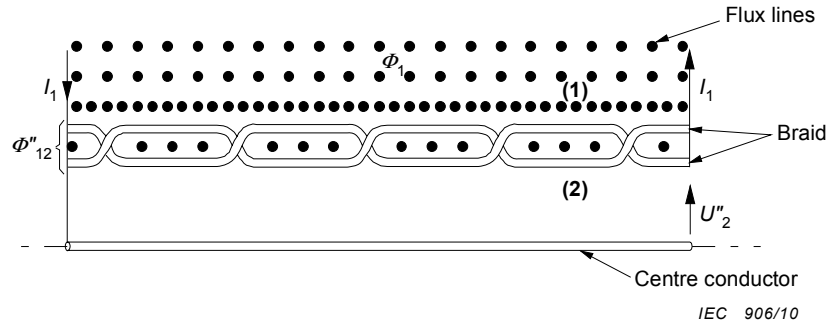


Figure 14 – Magnetic coupling in the braid
Complete flux

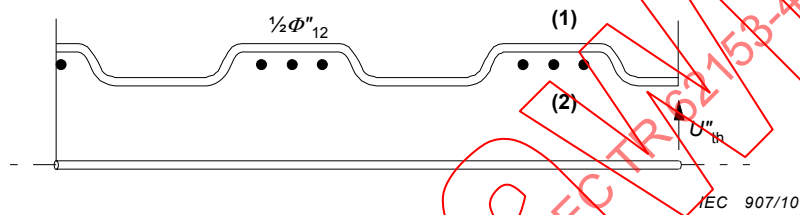


Figure 15 – Magnetic coupling in the braid
Left-hand lay contribution

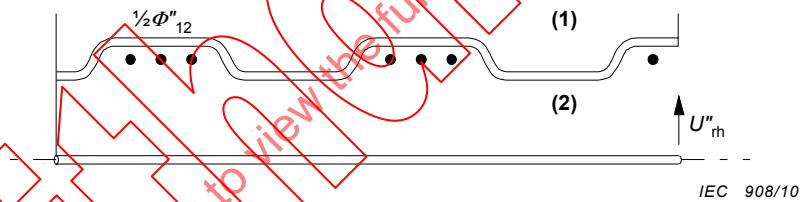


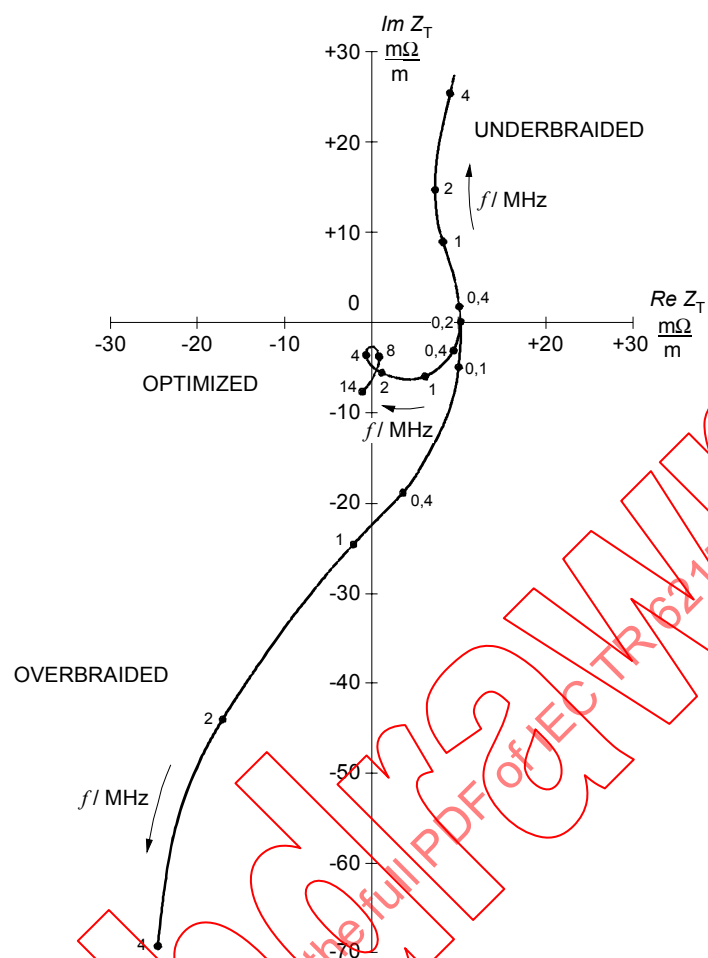
Figure 16 – Magnetic coupling in the braid
Right-hand lay contribution

Therefore it is necessary and unavoidable that Φ''_{12} is partly also in the inner circuit, Figure 14. Both the right hand (rh) (see Figure 16) and left hand (lh) lay (see Figure 15) of the braiding wires bring into the inner circuit (2) an equal disturbing voltage U''_2 induced by $\Phi''_{12} / 2$. The voltages are in parallel:

$$U''_{rh} = U''_{lh} = U''_2 = \frac{1}{2}j\omega\Phi''_{12} \quad (24)$$

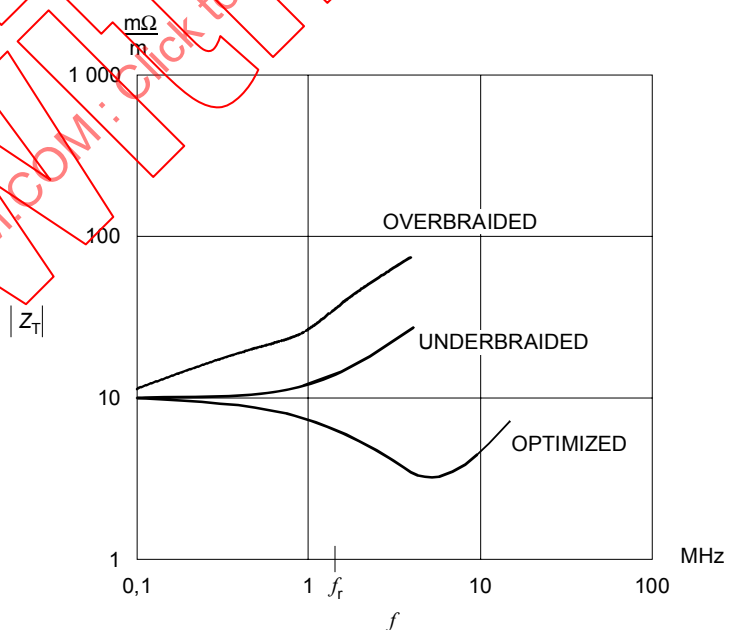
This phenomenon is similar to the "magnetic part" of the coupling through a homogeneous screen.

The two induced disturbing voltages oppose each other.



IEC 909/10

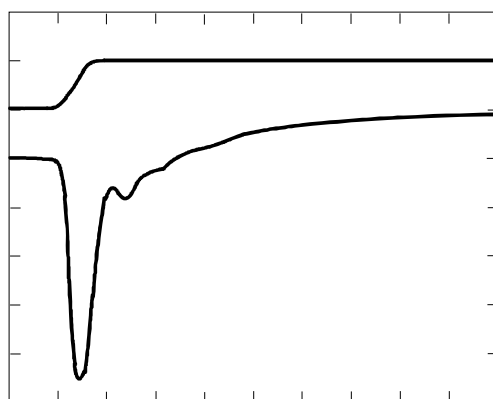
Figure 17 – Complex plane, $Z_T = \text{Re } Z_T + j \text{Im } Z_T$, frequency f as parameter



IEC 910/10

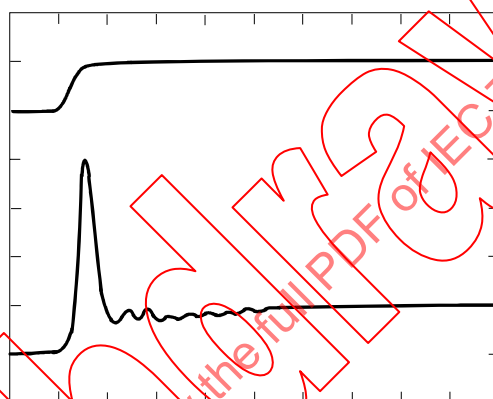
Figure 18 – Magnitude (amplitude), $|Z_T(f)|$

In Figure 17 and Figure 18 the d.c., resistance Z_T (d.c.), is set to the value of 10 $\text{m}\Omega/\text{m}$.



IEC 911/10

Figure 19a – Overbraided cable



IEC 912/10

Figure 19b – Underbraided cable

Top trace: Injection step current (100 mA/div)

Time base: 50 ns/div

Amplifier gain: 30 dB, therefore Z_T (time) = 12,5 mΩ/m/div

Lower trace: The height of the spike corresponds to

a) $-Z_T$ (3 MHz) = $-4,7 \times 12,5 \text{ m}\Omega/\text{m} = -59 \text{ m}\Omega/\text{m}$;

b) $-Z_T$ (3 MHz) = $+4 \times 12,5 \text{ m}\Omega/\text{m} = +50 \text{ m}\Omega/\text{m}$.

Figure 19 – Typical Z_T (time) step response of an overbraided and underbraided single braided outer conductor of a coaxial cable

Braid optimization is based on these important physical facts. Both leakage phenomena can be described by mutual inductances:

$$M'_{12} = \frac{\Phi'_{12}}{j\omega l_1} \quad (25)$$

$$M''_{12} = \frac{1}{2} \times \frac{\Phi''_{12}}{j\omega l_1} \quad (26)$$

Clearly it is possible to make braided-wire screens where either M'_{12} or M''_{12} are dominant or where they cancel each other. Therefore, underbraided, overbraided or optimized braids may be considered. Figure 17 shows measured transfer impedances in the complex plane of such screens and the main transfer impedance components of a braided screen can be observed. From the optimized case it can be concluded that at low frequencies the braid behaves approximately as a homogeneous tubular screen. The same can be concluded from Figure 18 where the transfer impedance amplitudes are shown as a function of frequency, but from Figure 18 it cannot be seen directly if the screen is underbraided or overbraided.

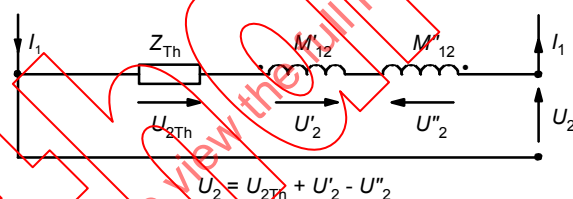
The transfer impedance of a braided wire screen consists of the following three main components (mentioned above).

- At low and medium frequencies the tubular screen coupling behaviour (Z_{Th}) varies with eddy currents and decreasing Z_T . In [2] it is stated that a good approximation for Z_{Th} is a tubular homogeneous screen [3] with the thickness of one wire diameter and the same d.c. resistance as the braid.
- The mutual inductance M'_{12} is related to direct leakage of the magnetic flux Φ'_{12} .
- The mutual inductance M''_{12} (negative) is related to the magnetic flux Φ''_{12} in the braid.

By adding these components a good approximation is obtained for the transfer impedance Z_T of a braided wire screen

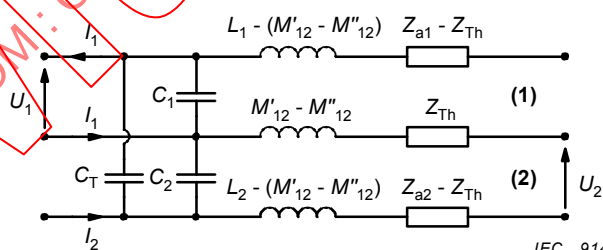
$$Z_T \approx Z_{Th} + j \omega (M'_{12} - M''_{12}) \quad (27)$$

and the first approximation of the equivalent circuit is shown in a) Figure 20.



IEC 913/10

Figure 20a – Contributions to the transfer impedance



IEC 914/10

Figure 20b – Significant elements of circuits (1) and (2)

Figure 20 – Z_T equivalent circuits of a braided wire screen

A more complete equivalent circuit where the through capacitance C_T and surface impedances Z_a of the braided cable are incorporated is shown in b) Figure 20. L_1 and L_2 are the (external) inductances of the outer and inner circuit.

Many attempts have been made to calculate the transfer impedance of a braided coaxial cable. Most of the literature [2, 4, 5] have concentrated on models of braided screens and calculation of direct leakage of the magnetic field induced by I_1 , and of M'_{12} . Satisfactory results have been achieved.

There exists very little literature [6], [7] on M''_{12} but the matter has been studied by IEC SC 46A/WG 1 and its successor TC 46/WG 5. Especially the calculation and stability of M''_{12} have been shown to be very problematic because of so many uncertain and unstable parameters, e.g. the resistance of the crossover points of the wires, which have an effect on the magnetic field distribution in the braid. Also the pressure of the jacket has an effect on the small space between the right hand lay and left-hand lay of the braided wires. Not to mention the number of wire ends per carrier and the braid angle and the tightness and optical coverage of the braid.

After understanding the magnetic coupling mechanisms it is not surprising that the transfer impedances of braided wire screens vary considerably and are unstable for many braid and cable constructions whether or not they are optimized. It is also clear that a perforated tube cannot be used as a model for a braided screen.

It is clear that a loose highly optimized braid can have a very unstable Z_T during bending, twisting and/or pressing. An overbraided screen with a high filling factor or optical cover normally has a (pure) negative transfer impedance at high frequencies because of a large M''_{12} coupling through the mutual "space" between the left and right lays of the braid in comparison with a small leakage through the braid M'_{12} . Pressure on the jacket would improve the screening performance by diminishing the mutual "space" and decrease the Z_T .

The manufacture of a good stable optimized cable requires the control of braid parameters such as:

- braid angle, tension (and lubricant) of the strands;
- number of strand in a spindle;
- wire diameter;
- plating;
- pressure of the jacket on the braid in manufacturing.

7 Test possibilities

7.1 General

A number of test procedures are used to test cables for their screening properties, some of which will be found in IEC standards. Each procedure has benefits for some users which for historical reasons may not be widely appreciated. Table 2 summarizes the test procedures available, some of which will be discussed here, with special reference to their applicability to cables, cable assemblies and connectors.

7.2 Measuring the transfer impedance of coaxial cables

All tests listed in Table 2 can be used on coaxial cables, but if a single test is needed to cover frequencies above and below 100 MHz, tests 1, 4, 7, 9 and 10 can be dismissed. Of the others, those with 's' under 'grouping' (column 3) have better intrinsic isolation between measuring and injection circuits, while in those with 'o' under grouping the injection circuit is unscreened. The difference is the line interchange referred to in 4.5 above. One benefit of an unscreened injection line is that better access may be obtained for inspection of the cable under test, which may be useful if the sample is in any way flawed. The two test methods with unscreened injection lines are test 3 and test 8. The latter, with its wide frequency coverage is recommended for future testing.

7.3 Measuring the transfer impedance of cable assemblies

Even with a restricted frequency range, many of the tests listed in Table 2 are not suited to tests on cable assemblies. Tests 1, 4, and 6 are unsuitable because an electrically short sample may be needed to achieve the upper frequencies, while test 10 is still limited to frequencies above 100 MHz. Tests with screened injection wires (test 2 and test 5) are difficult to set up due to the varying cross section of the assembly, a difficulty which also applies to

test 3. Such objections leave tests 7, 8 and 9. To set against its low (effective) upper frequency limit, with test 7 it is easy to distinguish between connector and cable contributions, so it is ideal in a diagnostic role. Test 9 works only above 30 MHz, which may be restrictive. Test 8 will require several measurements on each sample, as it is unreasonable to assume that a cable assembly has circular symmetry.

It is only fair to state that in any frequency domain test on cable assemblies where signal phase is not recorded, a test is only valid if the sample length is not varied (tests carried out on a sample of one length, cannot be used to assess a sample of another length – whether it be longer or shorter). Of the transfer impedance tests being discussed, only test 7 can be used in this way.

Multi-conductor cable assemblies are more complex, because the 'core' cannot be considered to be coaxial. A test for such cable assemblies has not yet been addressed.

7.4 Measuring the transfer impedance of connectors

In principle, all the tests in Table 2 can be used on coaxial connectors.

As with tests on cable assemblies, there is much benefit to be gained from using a test with an unscreened injection circuit, though other tests will remain in the standard, because they have become accepted. If it is possible to distinguish the screening of a connector from that of the attached cable, this will considerably ease the test procedure.

Multi-pin connectors are far more numerous and varied than coaxial connectors. However, non-circular connectors cannot be tested by the means implied by the test procedures of Table 2, though by suitable variation test 7 and test 10 would become appropriate. This problem is under study.

NOTE These methods give only an outline for measurement of symmetrical multicore cables, multipin connectors and cable assemblies made with these components.

The problems to address come from:

- a) the fact that a connector is electrically short, while the parameters of a cable are distributed, and it may be electrically long;
- b) multi-core cables rarely have circular symmetry. This applies both physically and to the signal paths on their conductors;
- c) most multi-pin connectors have no circular symmetry; nor are they equally spaced from other conductors, which might couple to them;
- d) economics will dictate that a cable assembly test should apply to other assemblies using the same components, even though of differing overall length.

7.5 Calculated maximum screening level

It is important to know the exact theoretical limitation of the test equipment. By knowing the limitations it is possible to calculate the maximum measurable screening effectiveness. This should be calculated to check the strengths and weaknesses of the test setup or even to optimize the test setup.

The following test equipment specifications are required for the calculation:

- minimum input (noise floor);
- maximum input;
- amplification/attenuation;
- maximum output.

Figure 21 gives a comparison of the different signal levels in a generic test setup. The maximum screening is the difference between the maximum obtainable input signal to the DUT and the minimum detectable signal from the DUT, in this case 131 dB. The noise floor level

(NL) of the measuring system must be low enough to allow the measurement. In this case lower than 122 dBm. Measurements at the noise floor result in a maximum error of 3 dB. When measured 6 dB above the noise floor the error is only about 1 dB.

The triaxial tube column is divided in two to show both the loss in the tube and the actual maximum screening.

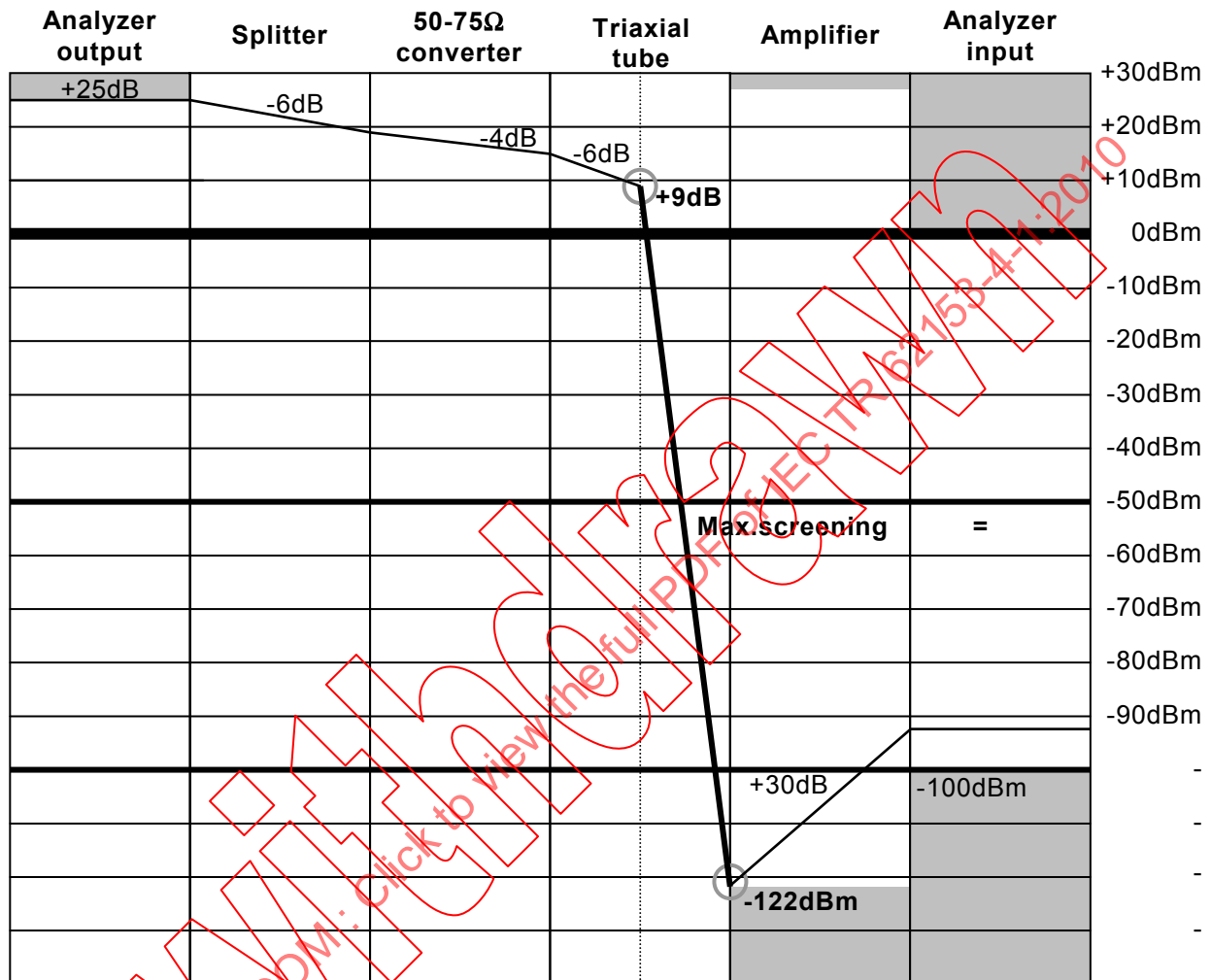


Figure 21 – Comparison of signal levels in a generic test setup

Taking into consideration the noise level of 1 Hz bandwidth at room temperature being -173 dBm, (increase $10 \times \log(\text{bandwidth})\text{dB}$) and adding the noise figure of the amplifier, we get the theoretical noise level of the test setup. Assuming that the amplifier in the Figure 21 example has a noise figure of 11 dB, we can then calculate, that the bandwidth (Δf) of the network analyzer shall be smaller than 10 kHz.

This can be expressed as a general formula:

$$NL = (-173 + F + 10 \times \log_{10} \Delta f) \quad (28)$$

where

N_L is the noise floor level of receiving side of the measuring system in dBm;

F is the noise figure of the pre amplifier in dB;

Δf is the bandwidth of the receiver in Hz.

IECNORM.COM: Click to view the full PDF of IEC TR 62153-4-1:2010

Withdrawn

Table 2 – Screening effectiveness of cable test methods for surface transfer impedance Z_T

Short title	Reference	Grouping (Note 1)	Frequency range		Injection N or F (Note 2)	Advantages or shortcomings
			Possible	Actually used		
1 IEC triaxial	Figure A9 of IEC 60096-1 Figure 44 of IEC 61196-1	kf s	d.c. – 50 MHz	10 kHz – 30 MHz	F	Rigid test rig
2 Terminated triaxial (Simons)	Figure A5 of IEC 60096-1	m s	10 kHz – 1 GHz	100 kHz – 500 MHz	N F	Flexible test jig relies on ferrites
3 Braid injection (Fowler)	AESS(TRG)71181 [9]	m o	d.c. – 500 MHz	10 kHz – 500 MHz	N F	Flexible test needs good screening on measuring system
4 Quadraxial	[10]	m s	100 kHz – 50 MHz	100 kHz – 1 GHz	N	Deep resonances make use above 50 MHz theoretically impossible. The test has been used for assessing screening at frequencies up to 1 GHz
5 Matched T triaxial (Staegar)	IEC 60169-1-3 [11] [12]	m s	1 kHz – 12 GHz	100 MHz – 10 GHz 10 kHz – 100 MHz	N F	Rigid test jig needs good screening
6 ERA triaxial (Smithers)	[13]	kf s	d.c. – 400 MHz	10 kHz – 300 MHz	F	Very short CUT requires amplifier or phase locked loop
7 Line injection (time domain)	IEC 60096-4-1 [14]	m o	d.c. – 100 MHz	1 kHz – 80 MHz (note 3)	N F	Very easy to use. Needs good screening in measuring amplifier
8 Line injection (frequency domain)	Figures 34 and 35 of IEC 61196-1 [8] [15]	m o	d.c. – 20 GHz	10 kHz – 3 GHz	N F	Flexible and cheap measuring set-up, equipment needs to be well shielded
9 Open screening attenuation test method (absorbing clamp)	Figures 50 to 52 of IEC 61196-1	m o	30 MHz – 2,5 GHz	30 MHz – 1 GHz 300 MHz – 2,5 GHz	N F	Poor sensitivity. Measuring of a_s is dependent on the surroundings
10 Reverberation chamber method	IEC 61726 [16]	kn kf	0,1 GHz →	0,3 GHz – 40 GHz	N & F	Flexible in use, but a complex and expensive computer controller with sophisticated test software needed
11 Shielded screening attenuation test method	[17] [18] (note 4)	m s	d.c. – 5 GHz	10 kHz – 3 GHz	F	High-sensitivity measurements can be made without a screened room
12 Open multipin connector screening test method	[19] [20]	o	d.c. – 1 GHz	10 kHz – 700 MHz	N	Low cost and flexible

Table 2 (continued)

Short title	Reference	Grouping (note 1)	Frequency range		Injection N or F (note 2)	Advantages or shortcomings
			Possible	Actually used		
13 Coupling attenuation measurements of balance cables and cable-assemblies						Under study
13.1 Current clamp injection method						Under study
13.2 Shielded triaxial test method						Under study
13.3 Absorbing clamp method						Under study

NOTE 1 Grouping by condition of 'primary circuit':
kn = short circuit at near end;
kf = short circuit at far end;
m = matched with characteristic impedance;
o = open on unscreened;
s = screened or shielded.

NOTE 2 N denotes near end feeding of primary relative to secondary circuit. F denotes far end feeding of primary relative to secondary circuit.

NOTE 3 Effective frequencies tested. Actually pulse with $T_R = 3,5$ ns and duration up to 160 μ s.

NOTE 4 Secondary circuit near end short circuited.

8 Comparison of the frequency response of different triaxial test set-ups to measure the transfer impedance of cable screens

8.1 General

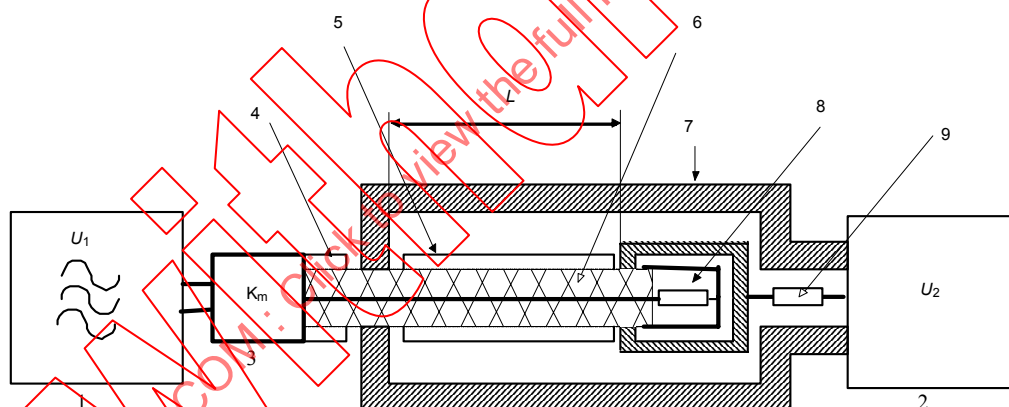
Different triaxial test set-ups for the measurement of the transfer impedance exist. One set-up is according to EN 50289-1-6 another according to IEC 61196-1. All of them are based on the same principle but are using different load conditions. In one method for example the cable under test is matched, while in the other the cable is short circuited at the far end. Furthermore, generator and receiver may be interchanged in the different set-ups. The following investigation analyses the frequency response of the different set-ups and their influence on the cut-off frequency up to which the transfer impedance could be measured.

8.2 Physical basics

8.2.1 Triaxial set-up

8.2.1.1 General

The triaxial set-up is of the “triple coaxial” form, see Figure 22 and Figure 23. A short length of the screen under test forms both, the inner conductor of the outer system and at the same time the outer conductor of the inner system. The coupling between the two coaxial systems is caused by the transfer impedance and the capacitive coupling admittance of the screen. The matching circuit, load resistor and series resistor are used to change the load conditions of the set-up. Also the generator and receiver may be interchanged between the different methods.

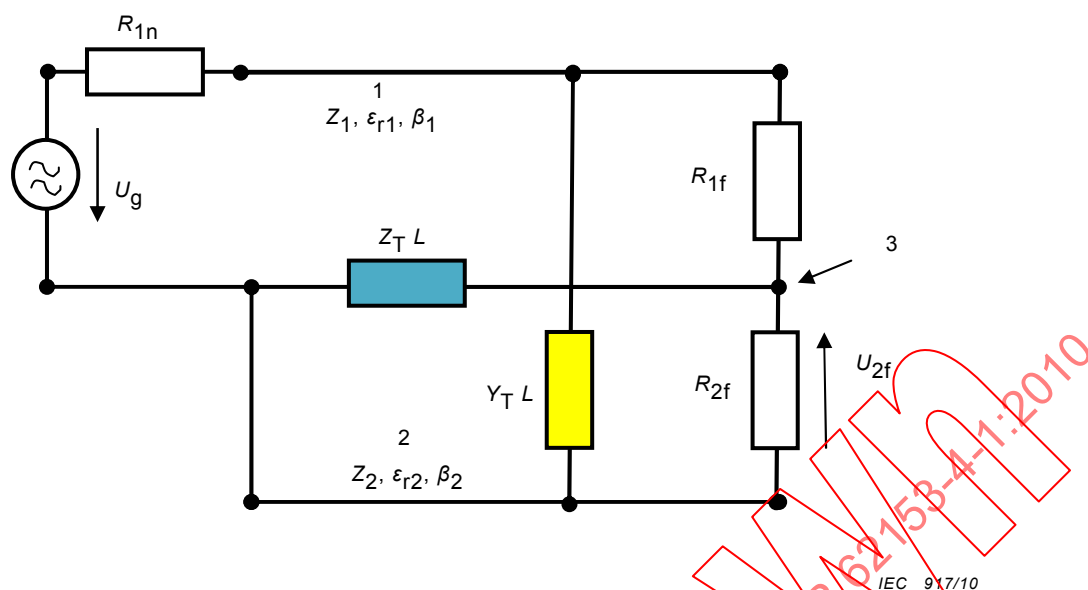


IEC 916/10

Key

- | | |
|---|------------------------|
| 1 Signal generator | 6 Cable screen |
| 2 Calibrated receiver or network analyzer | 7 Tube |
| 3 Matching circuit | 8 Terminating resistor |
| 4 Cable under test | 9 Series resistor |
| 5 Cable sheath | |

Figure 22 – Triaxial set-up for the measurement of the transfer impedance Z_T

**Key**

1	Inner circuit, cable
2	Outer circuit, tube
3	Screen
$Z_{1,2}$	Characteristic impedance of the inner circuit, cable, respectively outer circuit, tube
$\epsilon_{1,2}$	Dielectric permittivity of the inner circuit, cable, respectively outer circuit, tube
$\beta_{1,2}$	Phase constant of the inner circuit, cable, respectively outer circuit, tube
L	Coupling length
Z_T	Transfer impedance
Y_T	Capacitive coupling admittance
R_{1n}	Load resistance at the near end of the inner circuit, cable. Equal to the output impedance of the generator respectively input impedance of the receiver including an eventually used feeding resistor
R_{1f}	Load resistance at the far end of the inner circuit, cable. Depending on the used method either equal to the characteristic impedance of the cable or a short circuit.
R_{2f}	Load resistance at the far end of the outer circuit, tube. Equal to the output impedance of the generator respectively input impedance of the receiver including an eventually used feeding resistor
U_g	EMF of the generator
U_{2f}	Voltage at the far end of the outer circuit

Figure 23 – Equivalent circuit of the triaxial set-up**8.2.1.2 Load conditions of the different set-ups**

EN 50289-1-6 is using a method, where the cable under test and the far end of the secondary circuit are matched. The signal is fed to the cable under test and the disturbing voltage is measured at the far end of the outer circuit. A simplified method is to neglect the matching resistor at the far end of the outer circuit, which results in a higher dynamic range.

IEC 61196-1 (1995) describes two methods:

Method 1: Feeding through a resistance, where the signal is fed via a resistance into the outer circuit and the disturbing voltage is measured at the far end of the cable under test.

Method 2: Direct feeding, where the signal power is fed directly into the outer circuit and the disturbing voltage is measured at the far end of the cable under test.

With the revision of IEC 61196-1 (1995), the standard IEC 62153-4-3 has been published which also describes several methods:

Method A “Matched-Short” is equal to EN 50289-1-6.

Method B “Short-Short” is the double short circuited method, where the load resistance of the cable is replaced by a short circuit; thus having two short circuits in the set-up. One is at the near end of the outer circuit, (between the cable screen and the tube) and the other is at the far end of the cable. The advantage of this method is the simplification of the sample preparation. A short circuit is easier to make than to solder a resistor, especially if the sample is a multi-conductor cable. Furthermore the measurement sensitivity is improved. Compared to the “matched-short” method the dynamic range is improved by about 16 dB. In the “milked on braid” method an additional braid, the measuring braid, is pulled over the cable sheath instead of using the measuring tube. The advantage is, that the sample could be bend under test, however the preparation is more laborious than with the measuring tube.

The load conditions of the different methods are given in Table 3. The impedance of the outer circuit, Z_2 is varying with the diameter of the screen under test. Using the measuring tube Z_2 is in general higher, and in the “milked on braid” method Z_2 is lower, than the input impedance of the receiver.

Table 3 – Load conditions of the different set-ups

Method	Generator	Receiver	R_{in}/Z_1	R_{if}/Z_1	Z_2/R_{2f}
EN 50289-1-6					
Standard	IC	OC	1	1	0,71
simplified	IC	OC	1	1	1...5 depending on the tube diameter
IEC 61196-1					
Method 1: feeding through a resistance	OC	IC	1	1	0,71
Method 2: direct feeding	OC	IC	1	1	1...5 depending on the tube diameter
IEC 62153-4-3 Double short circuit methods					
With tube	OC	IC	1*	0	1...5 depending on tube diameter
With milked on braid	IC	OC	1*	0	0,1...0,4 depending on screen and sheath diameter of the cable
IC: inner circuit (cable under test) OC: outer circuit (tube) * only if the cable impedance is equal to the generator impedance. For other cable impedances the value may vary, e.g. 0,67 for cables with an impedance of 75 Ω .					

8.2.2 Coupling equations

The equations for the coupling between the inner circuit and outer circuit for any load conditions are described in [21] and [22]. By taking into account the short circuit at the near end of the outer circuit (between the cable screen and the measuring tube), neglecting the attenuation of the disturbing and disturbed line, assuming non ferromagnetic materials and introducing further variables, the following equations are defined.

$$\frac{u_{2f}}{u_q} = \frac{L}{R_{1f} + R_{1n}} \cdot [Z_T \cdot g + Z_F \cdot h] \quad (29)$$

$$g = \frac{1}{N} \cdot \frac{1}{1-n^2} \cdot \frac{j}{x} \cdot \{ r \cdot [\cos x - \cos nx] - j \cdot n \cdot \sin nx + j \cdot \sin x \} \quad (30)$$

$$h = \frac{1}{N} \cdot \frac{1}{1-n^2} \cdot \frac{j}{x} \cdot \{ n \cdot r \cdot [\cos x - \cos nx] - j \cdot \sin nx + j \cdot n \cdot \sin x \} \quad (31)$$

$$N = \left\{ \cos x + \frac{j \cdot \sin x}{r+w} \cdot [1+r \cdot w] \right\} \cdot \{ \cos nx + j \cdot v \cdot \sin nx \} \quad (32)$$

$$x = \beta_1 \cdot L = 2\pi \cdot \frac{L}{\lambda_1} \quad (33)$$

$$n = \frac{\beta_2}{\beta_1} = \frac{\lambda_1}{\lambda_2} = \frac{\sqrt{\epsilon_{r2}}}{\sqrt{\epsilon_{r1}}} \quad (34)$$

$$r = \frac{R_{1f}}{Z_1} \quad (35)$$

$$v = \frac{Z_2}{R_{2f}} \quad (36)$$

$$w = \frac{R_{1n}}{Z_1} \quad (37)$$

The factors g and h (see Equations 30 and 31) describe the frequency response of the test set-up. At low frequencies, when $\lambda \gg L$, the factors g and h are equal to 1. However with increasing frequency the factors g and h start to oscillate and thus also the measurement results. The maximum frequency to which the transfer impedance could be measured without oscillations, caused by the set-up, is defined as the 3 dB deviation from the linear interpolation of the measurement results. Or in other words if the factor g respectively h become $>\sqrt{2}$ respectively $<1/\sqrt{2}$.

8.3 Simulations

8.3.1 General

For the following investigations simulations have been chosen rather than a pure mathematical solution because they are easier to grasp and clearly illustrate the differences in the set-ups given in Table 4. In general the capacitive coupling can be neglected compared to the magnetic coupling ($Z_F \ll Z_T$), i.e. the cut-off frequency is mainly determined by the frequency behaviour of the factor g . Thus the following simulations are limited to the factor g .

Due to the reciprocity of the materials it is possible to interchange the generator and receiver without changing the results. Thus the standard EN 50289-1-6 method gives the same results as IEC 61196-1 method 1: “feeding through a resistance” and the simplified EN 50289-1-6 method gives the same results as IEC 61196-1 method 2: “direct feeding”.

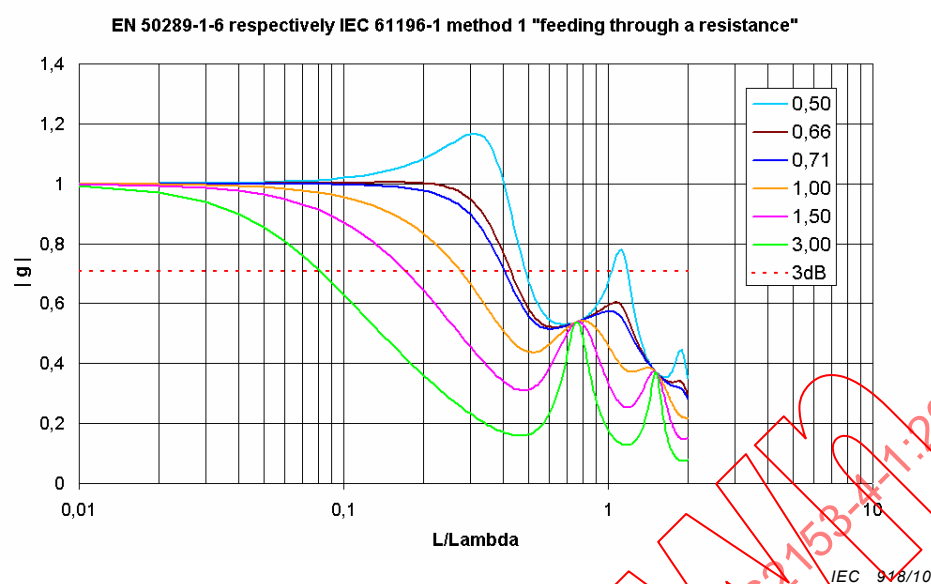
Table 4 – Parameters of the different set-ups

Method	$w=R_{1n}/Z_1$	$r=R_{1f}/Z_1$	$v=Z_2/R_{2f}$	$n=\sqrt{\varepsilon_{r2}}/\sqrt{\varepsilon_{r1}}$
EN 50289-1-6, IEC 62153-4-3 method A				
Standard	1	1	0,71	0,66 (0,45)...0,91
Simplified	1	1	1...5 depending on the tube diameter	
IEC 61196-1				
Method 1: feeding through a resistance	1	1	0,71	0,66 (0,45)...0,91
Method 2: direct feeding	1	1	1...5 depending on the tube diameter	
IEC 62153-4-3 Double short circuit methods				
With tube	1*	0	1...5 depending on tube diameter	0,66 (0,45)...0,91
With milked on braid	1*	0	0,1...0,4 depending on screen and sheath diameter of the cable	1,02...2,0
* only if the cable impedance is equal to the generator impedance. For other cable impedances the value may vary, e.g. 0,67 for cables with an impedance of 75 Ω.				

In the tube methods the factor n is given by the dielectric permittivity of the cable (inner circuit) as the dielectric permittivity of the outer circuit is nearly independent on the sheath material and can be assumed to be 1. However in the “milked on braid method” the factor n is dependent on both the dielectric permittivity of the cable insulation and the sheath, as the “measuring braid” is directly put on the sheath of the sample. The values for the factor n are given for typical insulation materials (PE, foam PE, PTFE...). The values in brackets are given for an insulation material of PVC, which may be used in multi-pair/conductor cables. For the “milked on braid” method typical combinations of insulation and sheath materials (PE/PVC, PE/LSZH, PTFE/FEP...) are taken into account, resulting in a value $n > 1$.

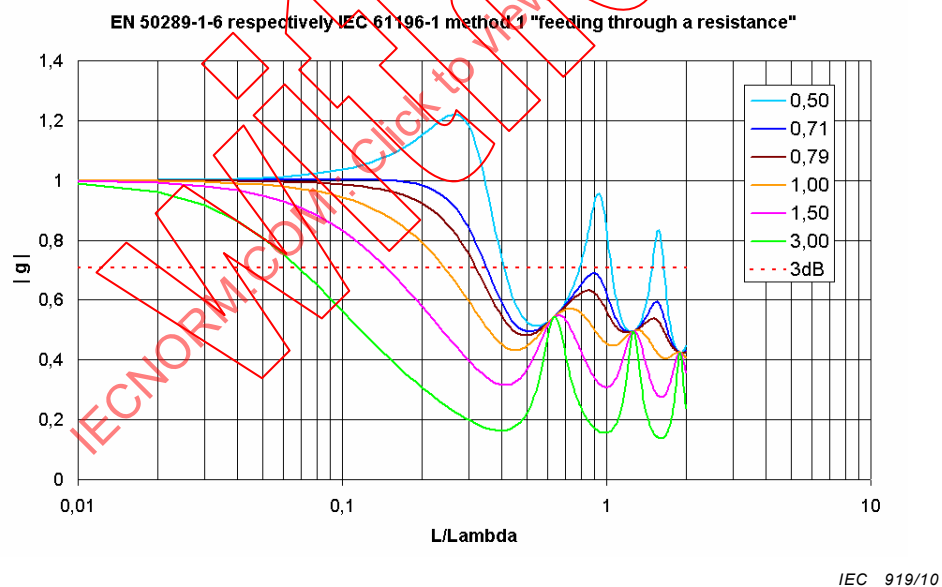
8.3.2 Simulation of the standard and simplified methods according to EN 50289-1-6, IEC 61196-1 (method 1 and 2) and IEC 62153-4-3 (method A)

In EN 50289-1-6, IEC 61196-1 method 1: “feeding through a resistance” and IEC 62153-4-3 method A: “Matched-Short” the factor $v=Z_2/R_{2f}$ is specified at $1/\sqrt{2}$. The simulations below show that this factor is a good compromise with respect to the maximum frequency to which the transfer impedance could be measured.

**Key**

Coloured lines correspond to indicated factors of $v=Z_2/R_{2f}$

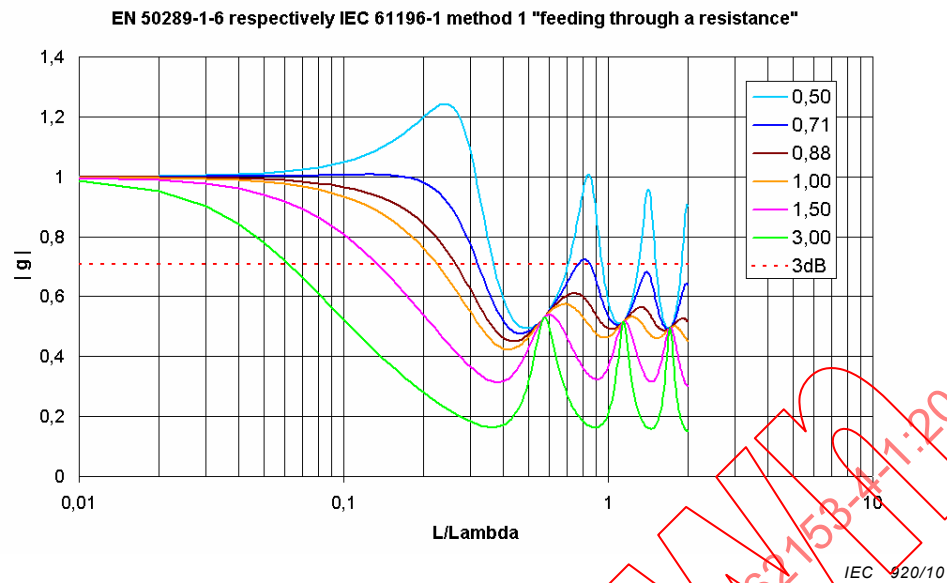
Simulation parameters		
ϵ_{r1}	ϵ_{r2}	n
2,3 (solid PE)	1,0	0,569

Figure 24 – Simulation of the frequency response for g **Key**

Coloured lines correspond to indicated factors of $v=Z_2/R_{2f}$

Simulation parameters		
ϵ_{r1}	ϵ_{r2}	n
1,6 (foam PE)	1,0	0,791

Figure 25 – Simulation of the frequency response for g

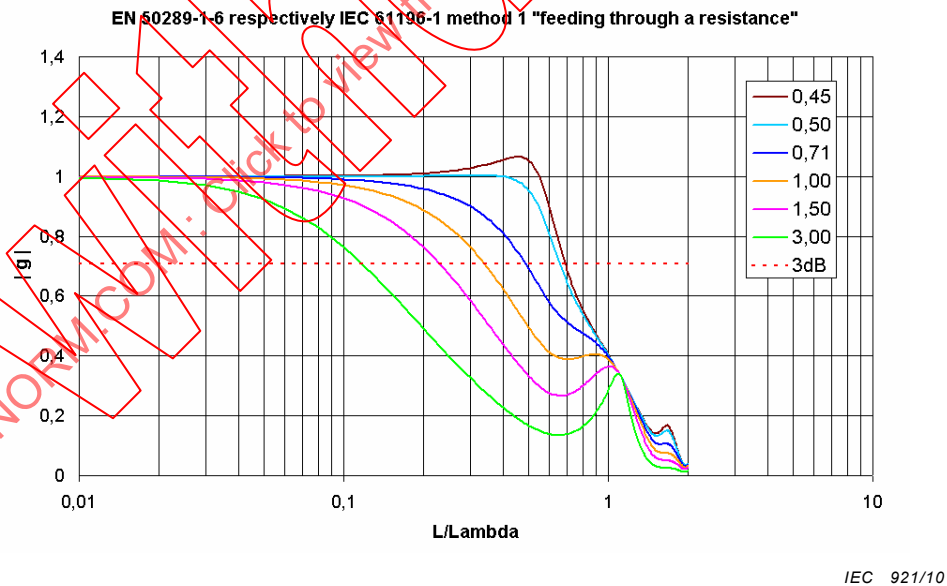


Key

Coloured lines correspond to indicated factors of $v=Z_2/R_{2f}$

Simulation parameters		
ϵ_{r1}	ϵ_{r2}	n
1,3 (foam PE)	1,0	0,877

Figure 26 – Simulation of the frequency response for g



Key

Coloured lines correspond to indicated factors of $v=Z_2/R_{2f}$

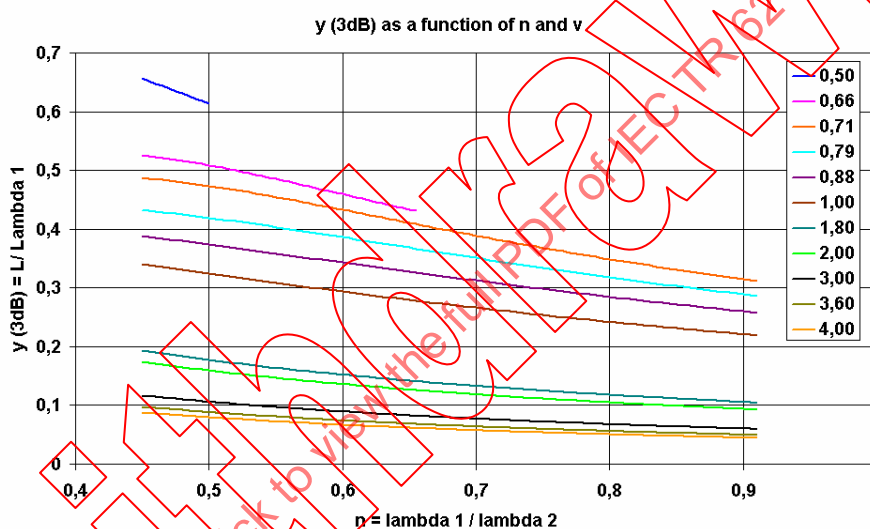
Simulation parameters		
ϵ_{r1}	ϵ_{r2}	n
5 (PVC)	1,0	0,447

Figure 27 – Simulation of the frequency response for g

The highest frequencies (respectively shortest wavelengths) are obtained if the factor $v=1/\sqrt{2}$ respectively $v=n$ whichever is smaller. In Figure 24 and Figure 27 the highest frequency is obtained for $v=n$ ($=0,659$ respectively $0,447$). But in Figure 25 and Figure 26 the highest frequency is obtained for $v=1/\sqrt{2}=0,71$. Below that value, the factor g is overshoots, i.e. becomes higher than one. Above that value, the cut-off frequency is decreasing.

Figure 28 gives the calculated, by iteration, 3 dB cut-off wavelength (L/λ_1) at which the factor $|g|$ becomes $1/\sqrt{2}$. The graph is given as a function of the factor $n=\sqrt{\epsilon_{r2}}/\sqrt{\epsilon_{r1}}$ and for different factors $v=Z_2/R_{2f}$. The curves show a linear behaviour and could be interpolated by straight line.

This has been done in Figure 29 for $v=1/\sqrt{2}$, $v=1$, $v=1,8$ and $v=3,6$. The factor $v=1/\sqrt{2}$ corresponds to the set-up according to EN 50289-1-6, IEC 61196-1 method 1 "feeding through a resistance" and IEC 62153-4-3 method A "Matched-Short". The other values of the factor v correspond to the simplified set-up, i.e. direct feeding. For common diameters of the measuring tube (around 40 mm) and common cable screen diameter (2 mm to 9 mm) the impedance in the outer circuit is 90 Ω to 180 Ω . Thus, for direct feeding resulting in $v=1,8 \dots 3,6$.



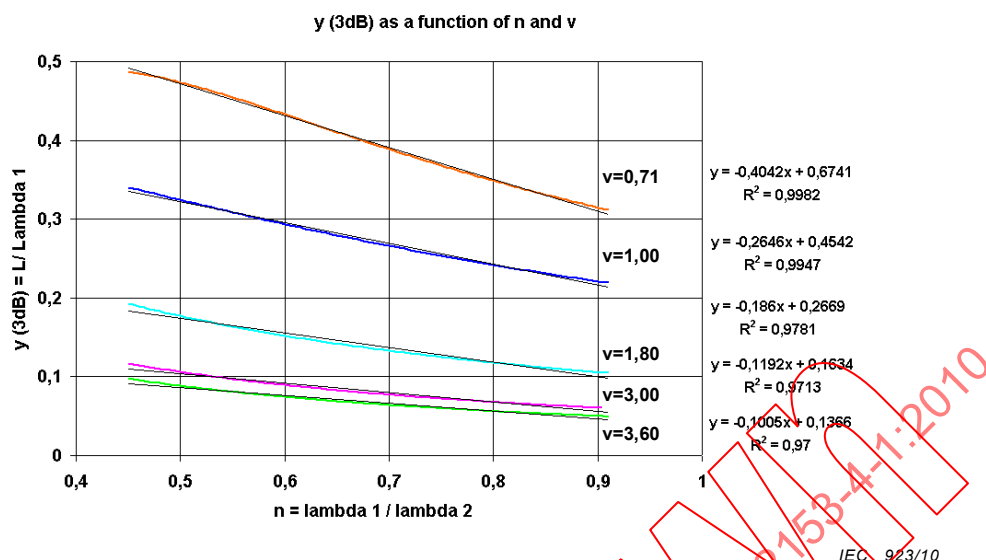
IEC 922/10

Key

Coloured lines correspond to indicated factors of $v=Z_2/R_{2f}$

Figure 28 – Simulation of the 3 dB cut off wavelength (L/λ_1)

The graphs for $v=0,5$ and $v=0,66$ are only given for n up to 0,5 respectively 0,66 because otherwise the factor g overshoots as described above.



Key

Coloured lines correspond to indicated factors of $v = Z_2 / R_{2f}$

Figure 29 – Interpolation of the simulated 3 dB cut off wavelength (L/λ_1)

The linear interpolation equation is used to derive an equation to calculate the cut-off frequency length product up to which the transfer impedance could be measured in a given triaxial test set-up.

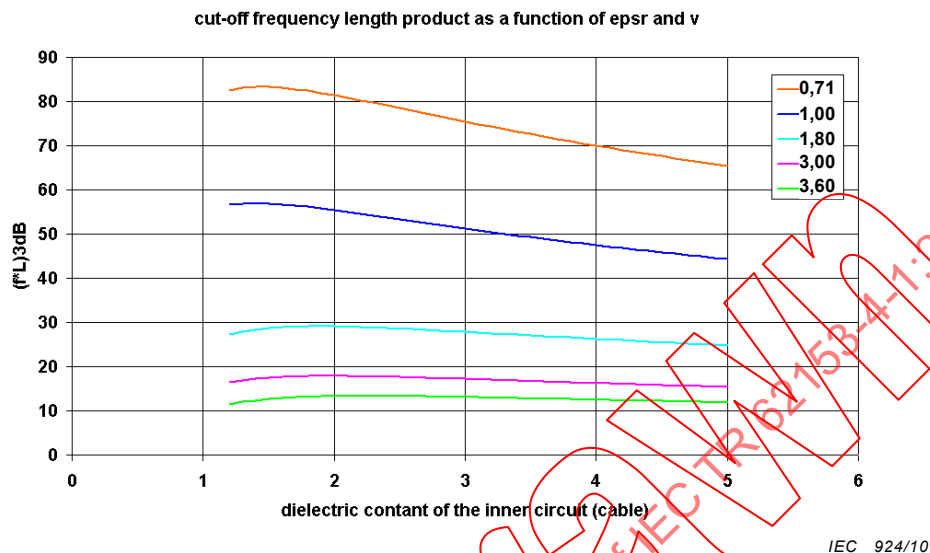
Table 5 – Cut-off frequency length product

Triaxial Test Set-up	v	Cut-off equation
EN 50289-1-6 IEC 61196-1 method 1 "feeding through a resistance" IEC 62153-4-3 method A "matched short"	$v=1/\sqrt{2}$	$(f \cdot L)_{3 \text{ dB}} \approx \left[\frac{200}{\sqrt{\epsilon_{r1}}} - \frac{120}{\epsilon_{r1}} \right] \cdot \text{MHz} \cdot \text{m}$
Simplified EN 50289-1-6 IEC 61196-1 method 2 "direct feeding"	$v=1$	$(f \cdot L)_{3 \text{ dB}} \approx \left[\frac{135}{\sqrt{\epsilon_{r1}}} - \frac{80}{\epsilon_{r1}} \right] \cdot \text{MHz} \cdot \text{m}$
	$v=1,8$	$(f \cdot L)_{3 \text{ dB}} \approx \left[\frac{80}{\sqrt{\epsilon_{r1}}} - \frac{55}{\epsilon_{r1}} \right] \cdot \text{MHz} \cdot \text{m}$
	$v=3$	$(f \cdot L)_{3 \text{ dB}} \approx \left[\frac{50}{\sqrt{\epsilon_{r1}}} - \frac{35}{\epsilon_{r1}} \right] \cdot \text{MHz} \cdot \text{m}$
	$v=3,6$	$(f \cdot L)_{3 \text{ dB}} \approx \left[\frac{40}{\sqrt{\epsilon_{r1}}} - \frac{30}{\epsilon_{r1}} \right] \cdot \text{MHz} \cdot \text{m}$

The equations given in Table 5 are drawn in the graphs of Figure 30.

For example if a cable with a PE insulation – dielectric permittivity of, $\epsilon_{r1} = 2,3$, and a screen diameter of 3,5 mm is measured in a triaxial set-up according to EN 50289-1-6 or IEC 61196-1 method 1 "feeding through a resistance" with $v=0,71$, than the cut-off frequency length product is about 80 MHz m. Therefore for a coupling length of 0,5 m the maximum frequency to which the transfer impedance could be measured is around 160 MHz

If the same cable is measured in a triaxial set-up according to IEC 61196-1 method 2 “direct feeding” or the simplified set-up according to EN 50289-1-6 where $v=3$, then the cut-off frequency length product is about 18 MHz m. For a coupling length of 0,5 m the maximum frequency to which the transfer impedance could be measured is around 36 MHz

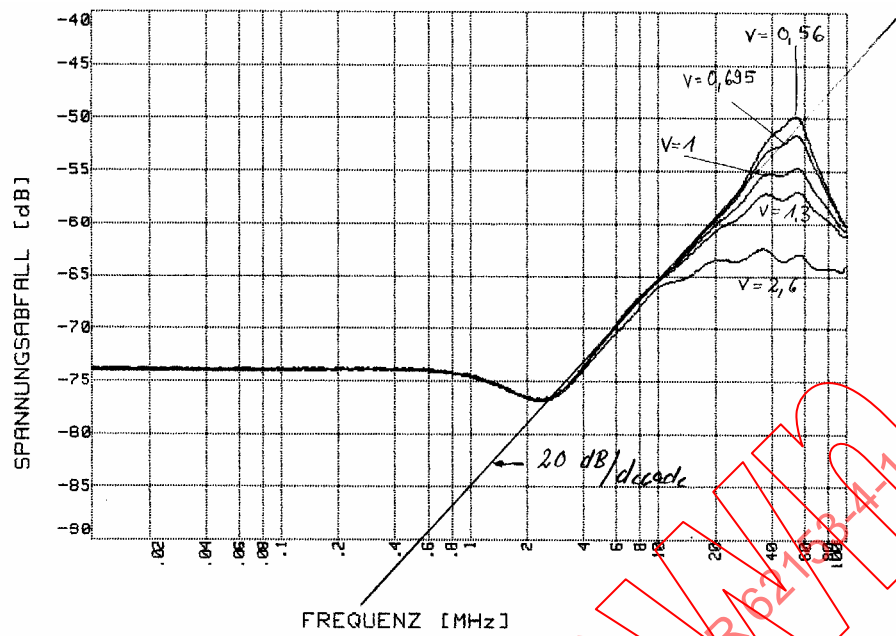


Key

Coloured lines correspond to indicated factors of $v=Z_2/R_{2f}$

Figure 30 – 3 dB cut-off frequency length product as a function of the dielectric permittivity of the inner circuit (cable)

Figure 31 and Figure 32 show the measurement results of the normalised voltage drop - i.e. the attenuation caused by the series resistor has been taken into account - in the triaxial set-up for different factors of v . Both figures show the results of the same screen design, however one with a solid PE insulation ($\epsilon_{r1}=2,3$) the other with a foam PE insulation ($\epsilon_{r1}=1,6$). The measurement results confirm the simulations. From the equations given above one gets cut-off frequency length products for $v=3$ of about 18 MHz m and for $v=1$ of about 55 MHz m for both the solid PE and the foam PE. This is also found from the measurement results.



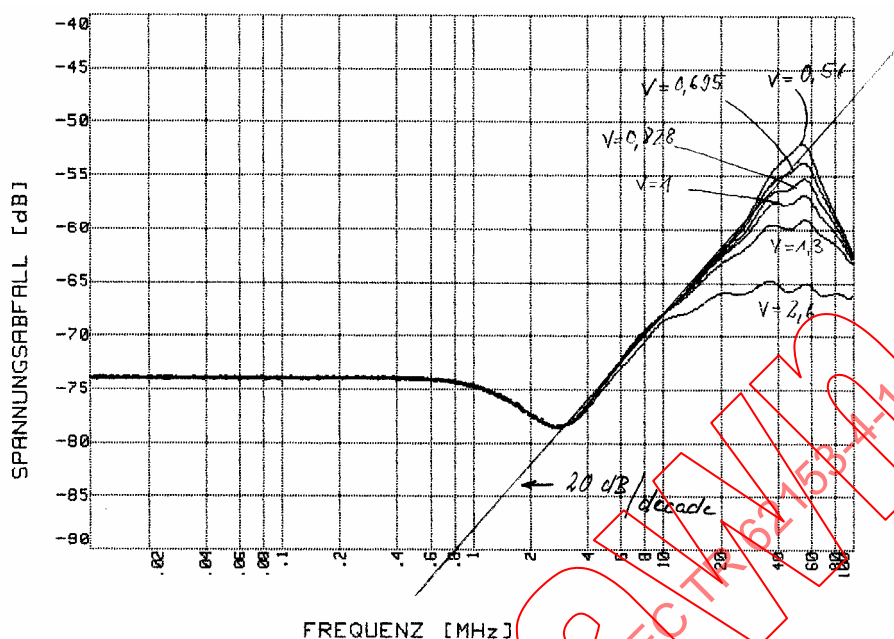
IEC 925/10

Key

Indicated lines correspond to factors of $v = Z_2/R_{2f}$

Measurement set-up parameters				
ϵ_{r1}	ϵ_{r2}	n	Z_2	L
2,3 (PE)	1,0	0,659	130 Ω	1 m

Figure 31 – Measurement result of the normalised voltage drop of a single braid screen in the triaxial set-up



IEC 926/10

KeyIndicated lines correspond to factors of $v = Z_2/R_{2f}$

Measurement set-up parameters				
ϵ_{r1}	ϵ_{r2}	n	Z_2	L
1,6 (foam PE)	1,0	0,791	130 Ω	1 m

Figure 32 – Measurement result of the normalised voltage drop of a single braid screen in the triaxial set-up

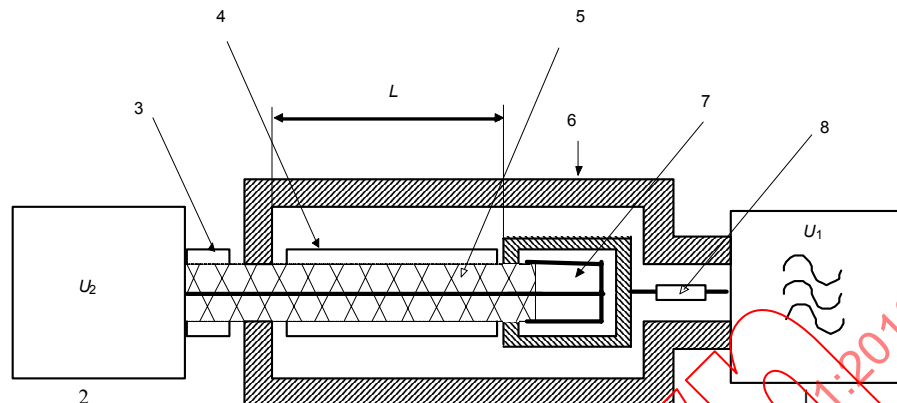
8.3.3 Simulation of the double short circuited methods

8.3.3.1 General

For the double short circuited methods one has either a measuring tube or a “milked on braid”. When using a measuring tube the dielectric permittivity of the outer circuit (tube) is nearly independent on the sheath material and could be assumed to be 1. However in the “milked on braid” method the dielectric permittivity is given by the sheath material. Thus the factor n is different for both methods. Also the impedance of the outer circuit is different for both methods. First due to the different dimensions second due to the different permittivities.

8.3.3.2 Simulation of the double short circuited method using a measuring tube

The double short circuited method using a measuring tube is shown in Figure 33. The outer circuit is fed over a fixed – i.e. the same value for all cable types – feeding resistor, the value of which is equal to the output impedance of the generator (e.g. 50 Ω). Thus the load impedance of the outer circuit at the far end is equal to 2 times the output impedance of the generator. The factor v is then only dependent on the diameters of the screen and of the measuring tube.



Key

- | | | | |
|---|--|---|-------------------------------|
| 1 | signal generator | 5 | able screen |
| 2 | alibrated receiver or network analyzer | 6 | ube |
| 3 | able under test | 7 | hort circuit |
| 4 | able sheath | 8 | eries resistor (50 Ω) |

IEC 927/10

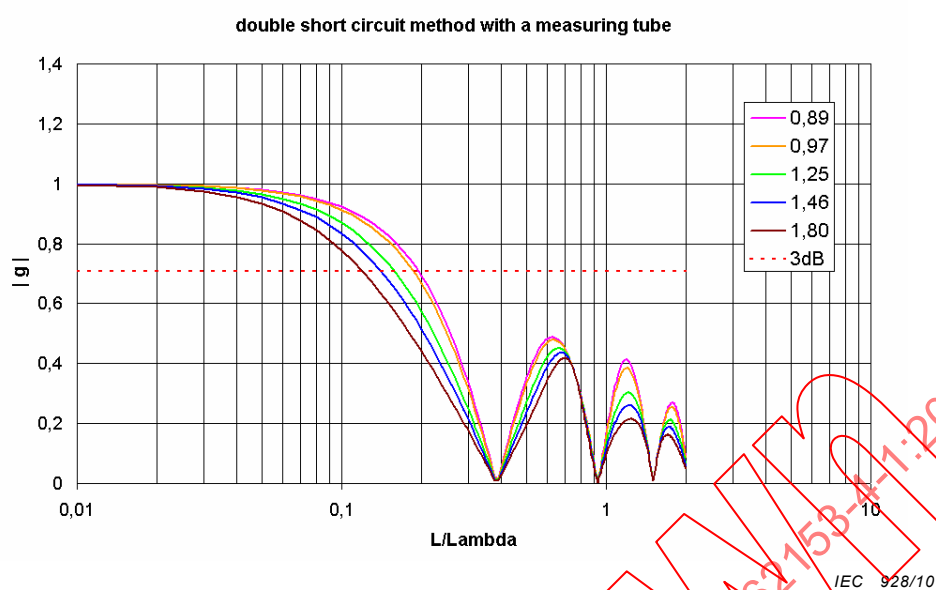
Figure 33 – Triaxial set-up (measuring tube), double short circuited method

Table 6 – Typical values for the factor ν , for an inner tube diameter of 40 mm and a generator output impedance of 50 Ω

Screen diameter mm	Z_2 Ω	$\nu = Z_2/R_{2f}$
9	89	0,89
8	97	0,97
5	125	1,25
3,5	146	1,46
2	180	1,80

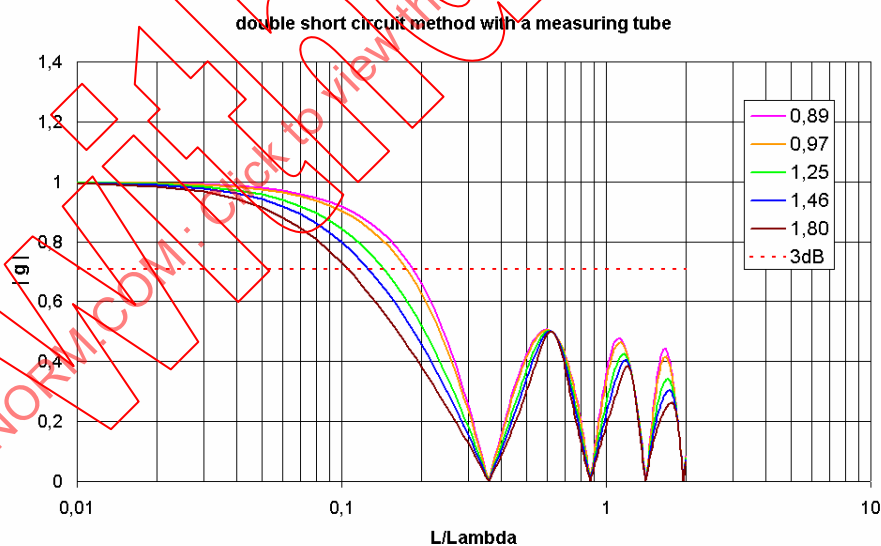
Those values have been used in the following simulations. The graphs in Figure 34 to Figure 37 show the simulated frequency response for different dielectric permittivities of the cable and for the different factors of ν given in Table 6.

Figure 38 plots the results of calculation by iteration for the 3 dB cut-off wavelength (L/λ_1) at which the factor $|g|$ becomes $1/\sqrt{2}$. The curves have then been interpolated by straight lines.

**Key**

Coloured lines correspond to indicated factors of $v=Z_2/R_{2f}$

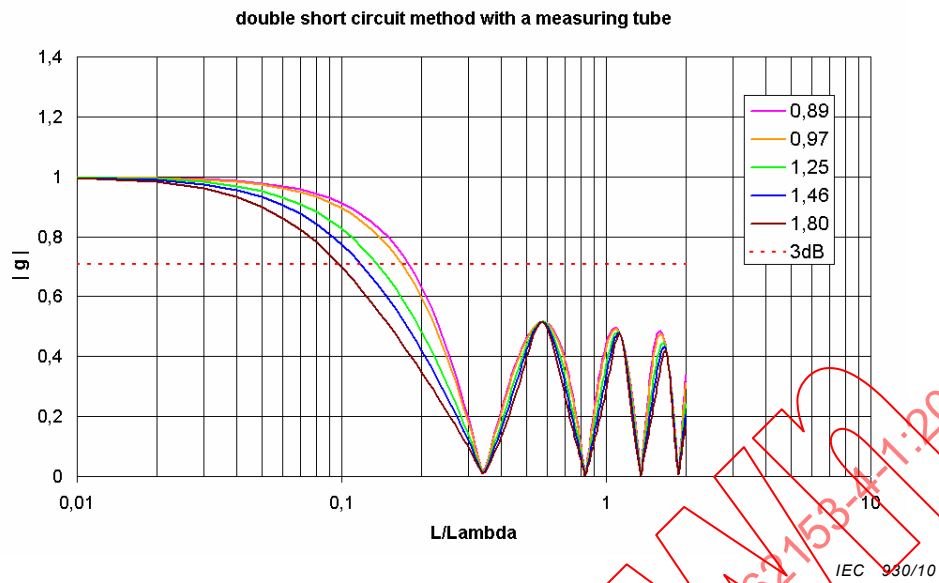
Simulation parameters		
ϵ_{r1}	ϵ_{r2}	n
2,3 (solid PE)	1,0	0,659

Figure 34 – Simulation of the frequency response for g **Key**

Coloured lines correspond to indicated factors of $v=Z_2/R_{2f}$

Simulation parameters		
ϵ_{r1}	ϵ_{r2}	n
1,6 (foam PE)	1,0	0,791

Figure 35 – Simulation of the frequency response for g

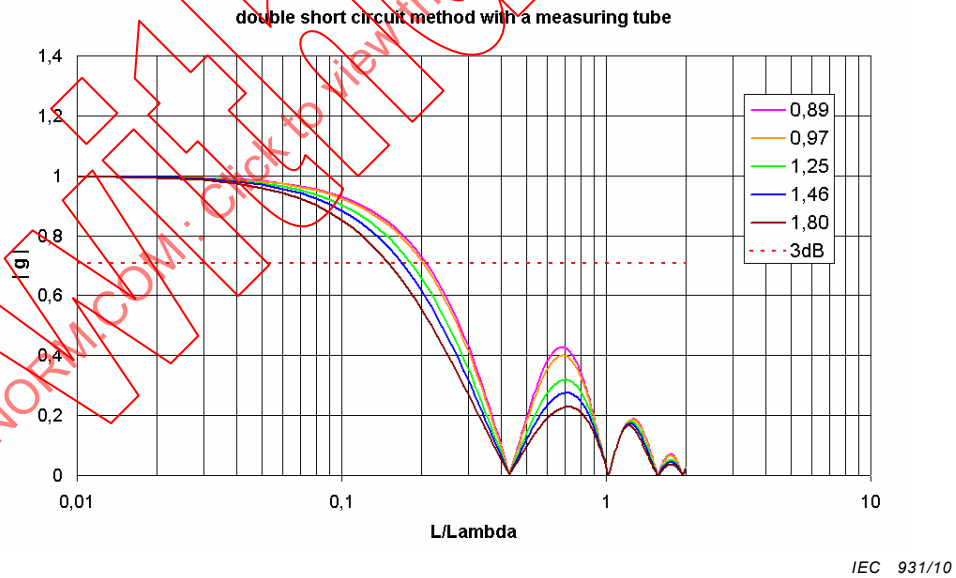


Key

Coloured lines correspond to indicated factors of $v=Z_2/R_{2f}$

Simulation parameters		
ϵ_{r1}	ϵ_{r2}	n
1,3 (foam PE)	1,0	0,877

Figure 36 – Simulation of the frequency response for g

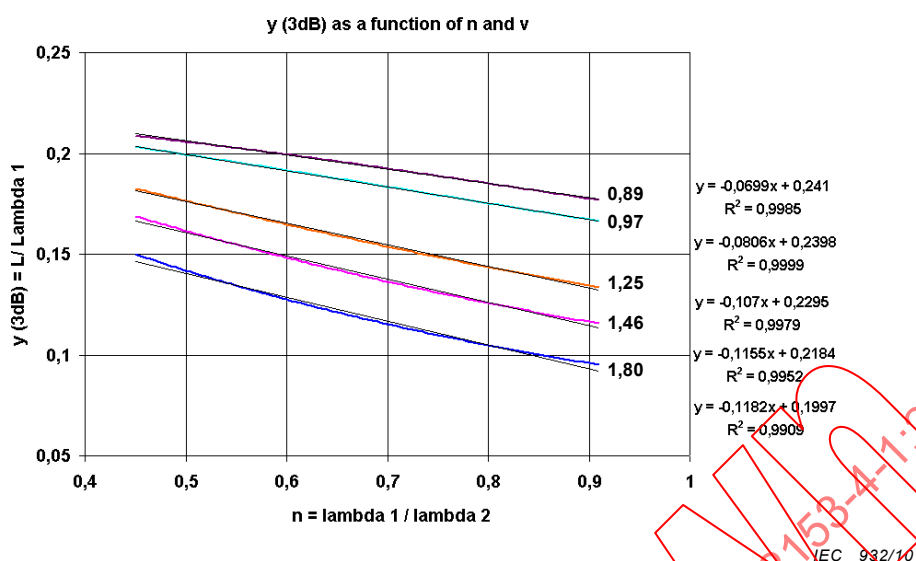


Key

Coloured lines correspond to indicated factors of $v=Z_2/R_{2f}$

Simulation parameters		
ϵ_{r1}	ϵ_{r2}	n
5 (PVC)	1,0	0,447

Figure 37 – Simulation of the frequency response for g



Key

Coloured lines correspond to indicated factors of $v = Z_2 / R_{2f}$

Figure 38 – Interpolation of the simulated 3 dB cut off wavelength (L/λ_1)

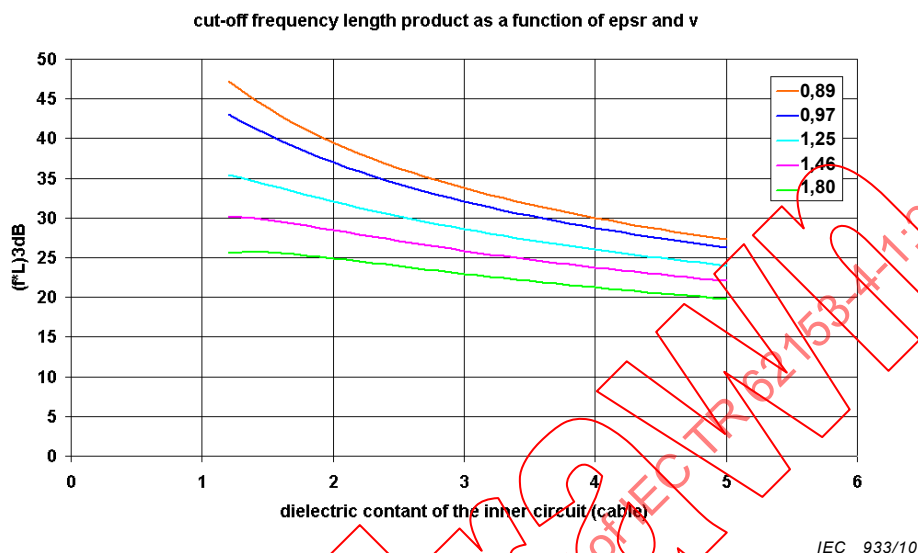
From the found linear interpolation one can derivate following equations to calculate the cut-off frequency length product, to which the transfer impedance could be measured in the “double short circuit” triaxial set-up using a measuring tube.

Table 7 – Cut-off frequency length product

$v=0,89$	$(f \cdot L)_{3 \text{ dB}} \approx \left[\frac{70}{\sqrt{\epsilon_{r1}}} - \frac{20}{\epsilon_{r1}} \right] \cdot \text{MHz} \cdot \text{m}$
$v=0,97$	$(f \cdot L)_{3 \text{ dB}} \approx \left[\frac{70}{\sqrt{\epsilon_{r1}}} - \frac{25}{\epsilon_{r1}} \right] \cdot \text{MHz} \cdot \text{m}$
$v=1,25$	$(f \cdot L)_{3 \text{ dB}} \approx \left[\frac{68}{\sqrt{\epsilon_{r1}}} - \frac{32}{\epsilon_{r1}} \right] \cdot \text{MHz} \cdot \text{m}$
$v=1,46$	$(f \cdot L)_{3 \text{ dB}} \approx \left[\frac{65}{\sqrt{\epsilon_{r1}}} - \frac{35}{\epsilon_{r1}} \right] \cdot \text{MHz} \cdot \text{m}$
$v=1,80$	$(f \cdot L)_{3 \text{ dB}} \approx \left[\frac{60}{\sqrt{\epsilon_{r1}}} - \frac{35}{\epsilon_{r1}} \right] \cdot \text{MHz} \cdot \text{m}$

The equations given in Table 7 are plotted in the graphs of Figure 39. For example if a cable with a PE insulation – dielectric permittivity of $\epsilon_{r1}=2,3$ – is measured in a triaxial set-up with $v=1,46$ (screen diameter=3,5 mm, tube diameter =40 mm), then the cut-off frequency length product is about 27 MHz m.: i.e. for a coupling length of 0,5 m the maximum frequency to which the transfer impedance could be measured is around 60 MHz. If the same cable is measured in a triaxial set-up according to IEC 61196-1 method 2 “direct feeding” or the simplified set-up according to EN 50289-1-6 where $v=3$, then the cut-off frequency length product is about 18 MHz m: i.e. for a coupling length of 0,5 m the maximum frequency to which

the transfer impedance could be measured is around 36 MHz. That is to say, that the double short circuit method (using a measuring tube) facilitates the sample preparation, has a 6 dB higher dynamic range and also allows to measure the transfer impedance up to higher frequencies, compared to the simplified EN 50289-1-6 or IEC 61196-1 method 2 “direct feeding”.



Key

Coloured lines correspond to indicated factors of $v = Z_2 / R_{2f}$

Figure 39 – 3 dB cut-off frequency length product as a function of the dielectric permittivity of the inner circuit (cable)

8.3.3.3 Simulation of the double short circuited method using a “milked on braid”

In the “milked on braid” method, a measuring braid is used instead of a measuring tube. The measuring braid is put directly over the sheath of the sample. Thus the dielectric permittivity of the outer circuit is given by the dielectric permittivity of the sheath ($\epsilon_{r2} = 2 \dots 5$), and the impedance of the outer circuit is given by the dielectric constant and the diameter over the sheath of the sample.

In this method the inner circuit is fed over a 10 dB attenuation pad instead of a 50 Ω feeding resistor while using a measuring tube. However, using a 10 dB attenuation pad instead of a feeding resistor doesn't affect the cut-off frequency, as described below.

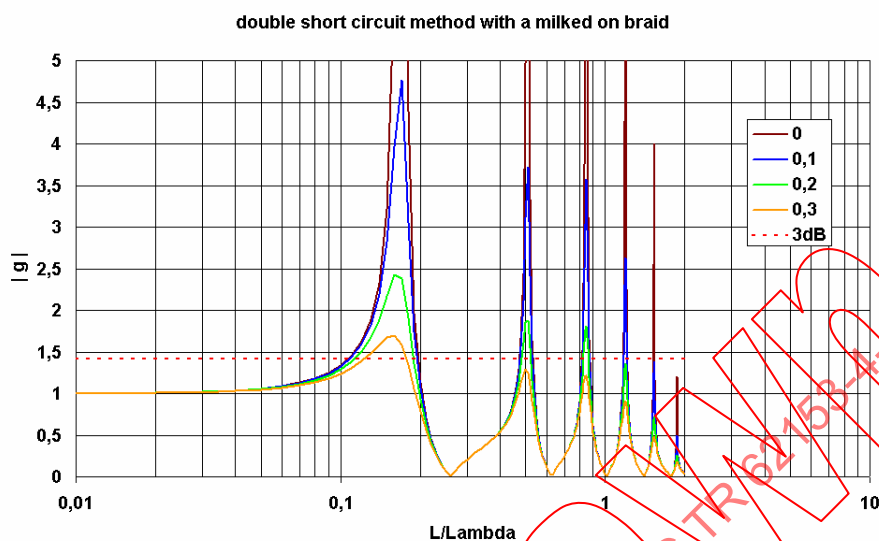
For cable screen diameters between 1 mm...10 mm, sheath thickness between 0,2 mm...1 mm and ϵ_{r2} between 2...5 the impedance in the outer circuit is between 5 Ω ...20 Ω , i.e. v between 0,1...0,4.

A closer look on the coupling equations (Equations 29 to Equation 37) shows, that for small values of the factor v and at low frequencies the frequency response of the test set-up (factor g) becomes nearly independent of it. The worst case with respect to the 3 dB cut-off is reached if $v=0$. This is drawn out in the equations below and in Figure 40. Thus in the following the simulations are done for $v=0$.

$$N = \left\{ \cos x + \frac{j \cdot \sin x}{r + w} \cdot [1 + r \cdot w] \right\} \cdot \{ \cos nx + j \cdot v \cdot \sin nx \}$$

for small values of v , i.e. $v \ll 1$ and low frequencies, i.e. $x \ll 1$ one gets

$$N = \left\{ \cos x + \frac{j \cdot \sin x}{r + w} \cdot [1 + r \cdot w] \right\} \cdot \left\{ e^{j \cdot nx} - j \cdot (1 - v \cdot \sin nx) \right\} \approx \left\{ \cos x + \frac{j \cdot \sin x}{r + w} \cdot [1 + r \cdot w] \right\} \cdot \left\{ e^{j \cdot nx} - j \right\}$$



IEC 934/10

Key

Coloured lines correspond to indicated factors of $v = Z_2/R_{2f}$

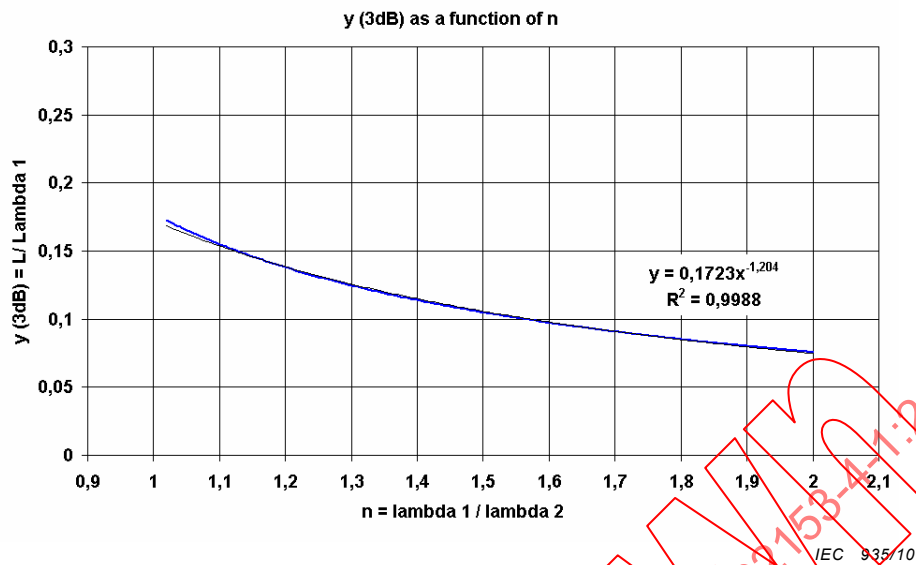
Simulation parameters		
ϵ_{r1}	ϵ_{r2}	n
2,3 (PE)	5 (PVC)	1,474

Figure 40 – Simulation of the frequency response for g

Taking into account typical combinations of insulation and sheath materials (PE/PVC, PE/LSZH, PTFE/FEP...) one gets values for the factor n between 1,02...2. Those values in Table 8 have been used for the iteration of the 3 dB cut-off wavelength (L/λ_1) shown in Figure 41.

Table 8 – Material combinations and the factor n

ϵ_{r1}	ϵ_{r2}	$n = \sqrt{\epsilon_{r2}} / \sqrt{\epsilon_{r1}}$
2,3 (PE)	5 (PVC)	1,47
	3 (LSZH)	1,14
1,6 (foam PE)	5 (PVC)	1,77
	3 (LSZH)	1,37
1,3 (foam PE)	5 (PVC)	1,96
	3 (LSZH)	1,52
2,0 (PTFE)	2,1 (FEP)	1,02
1,3 (expanded PTFE)	2,1 (FEP)	1,27



Key

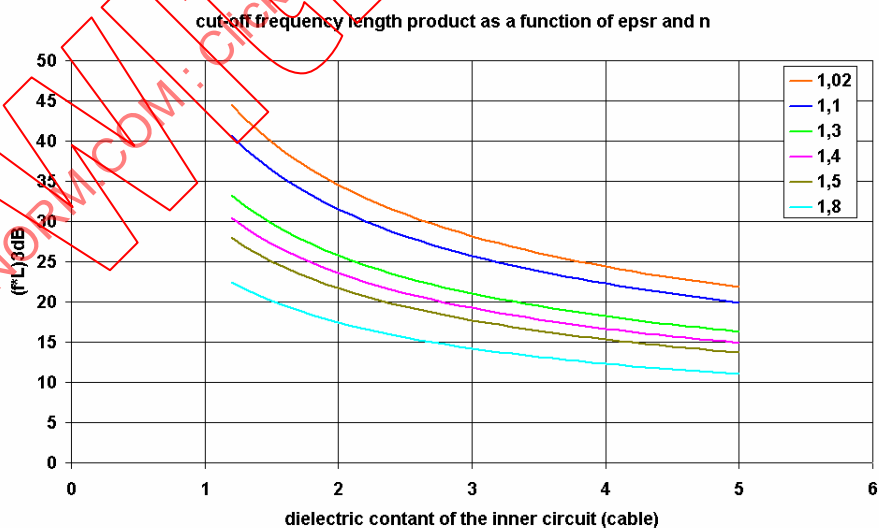
Plotted line is for $v = Z_2/R_{2f} \ll 1$

Figure 41 – Interpolation of the simulated 3 dB cut off wavelength (L/λ_1)

From the interpolation one can derive following equation given in Table 9 for the 3 dB cut-off frequency length product. The equation in Table 9 is plotted in Figure 42.

Table 9 – Cut-off frequency length product

$v \ll 1$	$(f \cdot L)_{3\text{ dB}} \approx \left[\frac{50 \times n^{-1,204}}{\sqrt{\epsilon_{r1}}} \right] \cdot \text{MHz} \cdot \text{m}$
-----------	--



Key

Coloured lines correspond to indicated factors of $n = \sqrt{\epsilon_{r2}}/\sqrt{\epsilon_{r1}}$, for $v = Z_2/R_{2f} \ll 1$

Figure 42 – 3 dB cut-off frequency length product as a function of the dielectric permittivity of the inner circuit (cable)

For example a cable with PE insulation and PVC sheath ($n=1,47$) with the dimensions of a RG 58 (screen diameter around 3,5 mm) measured with the “milked on braid” method results in a cut-off frequency length product of 20 MHz·m. The same cable measured in the double short circuit method with a measuring tube results in a cut-off length product of 27 MHz·m. If measured in the simplified EN 50289-1-6 method respectively one gets a cut-off frequency length product of 18 MHz·m. Thus the major advantage of the “milked on braid” method is, that it allows for bending of the sample under test.

8.4 Conclusion

The best compromise between a simple test set-up and the cut-off frequency is given for the “double short circuit” method using a measuring tube. It covers the usually required frequency range of 100 MHz (see Table 10) for the transfer impedance measurement (using a 30 cm tube) and has the highest dynamic range of all triaxial methods.

The “milked on braid” method has a limited frequency range, requires a long sample preparation but allows for bending of the sample under test.

The matched method according to EN 50289-1-6, IEC 62153-4-3 method A “matched-short” respectively IEC 61196-1 method 1 “direct feeding” has the highest cut-off frequency but also the lowest dynamic range. An additional error source in that method is the accuracy of the series resistor which might have unknown frequency behaviour and thus an unknown attenuation.

Table 10 – Cut-off frequency length product for some typical cables in the different set-ups

Cable type	Sheath	EN 50289-1-6 IEC 61196-1 method 1 IEC 62153-4-3 method A	Double short circuit method using a tube	Double short method using a milked on braid
RG 58 ($\epsilon_{r1}=2,3$)	PVC	80 MHz·m ($v=0,71$)	28 MHz·m ($v=1,46$)	20 MHz·m ($n=1,47$)
	LSZH			28 MHz·m ($n=1,14$)
Thin Ethernet ($\epsilon_{r1}=1,6$)	PVC	83 MHz·m ($v=0,71$)	30 MHz·m ($v=1,46$)	20 MHz·m ($n=1,77$)
	LSZH			28 MHz·m ($n=1,37$)
RG 214 ($\epsilon_{r1}=2,3$)	PVC	80 MHz·m ($v=0,71$)	35 MHz·m ($v=0,97$)	20 MHz·m ($n=1,47$)
	LSZH			28 MHz·m ($n=1,14$)
RG 8 ($\epsilon_{r1}=1,3$)	PVC	83 MHz·m ($v=0,71$)	42 MHz·m ($v=0,97$)	20 MHz·m ($n=1,96$)
	LSZH			26 MHz·m ($n=1,52$)

9 Background of the shielded screening attenuation test method (IEC 62153-4-4)

9.1 General

In many cases, above all in the lower frequency range, the screening effectiveness of cables is described by the transfer impedance Z_T . It is, for an electrically short length of cable, defined (see Figure 43) as the quotient of the longitudinal voltage measured on the secondary side of the screen to the current in the screen, caused by a primary inducing circuit, related to unit length [23]. Although the transfer impedance Z_T covers only the galvanic and magnetic couplings it is common practice to use it also as a quantity which includes the effect of the coupling capacitance C_T through the cable screen [24]. In this case it is named equivalent transfer impedance Z_{TE} which includes the effects of galvanic, magnetic and capacitive coupling.

For the determination of the proper coupling capacitance there is, as standardised quantity, the capacitance coupling admittance Y_T . The coupling admittance, (see Figure 44) for an electrically short piece of cable, is defined as the quotient of the current in the screen caused by the capacitive coupling in the secondary circuit to the voltage in the primary circuit related to unit length [23].

With electrically short cables, where wave propagation can be neglected, the screening quantities related to unit length can directly be used to calculate an induced disturbing voltage. In the higher frequency range the implications get similar complicated as the transmission characteristics of a simple line, dependent on the impedance and admittance per unit length as well as on the terminating resistors.

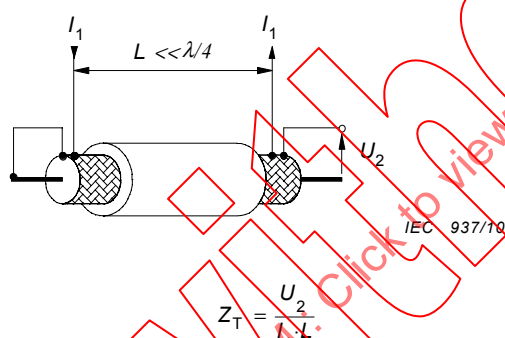


Figure 43 – Definition of transfer impedance

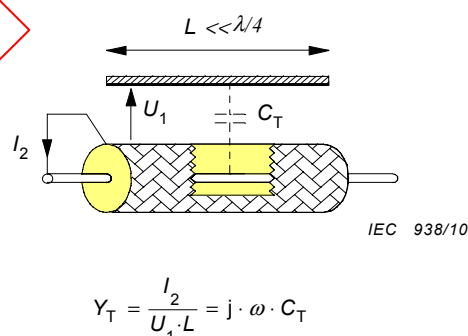


Figure 44 – Definition of coupling admittance

9.2 Objectives

It is desirable to measure and evaluate the screening efficiency of cable screens also in the wave propagation frequency range such that its characteristics can be directly applied. This requires a closer examination of the conditions of such applications.

In general, a system of electromagnetic induction consists of a transmission circuit in the cable, which is assumed to be fully defined, and of a surrounding transmission system, which is assumed to be universal with respect to the definition of cable screening. The screening effectiveness may be universally described by the maximum power output into the surroundings of the cable related to the power propagating in the cable. The power ratio is best expressed logarithmically as screening attenuation.

An often used procedure to determine the screening attenuation is the well known “absorbing clamp method” given in IEC 62153-4-5. The drawback of this method is, that the set-up requires relatively much space, does not exclude environmental effects - unless the measuring area is enclosed in a shielded cabin -, and that the available absorbing clamp transformers considerably limit the measurement sensitivity.

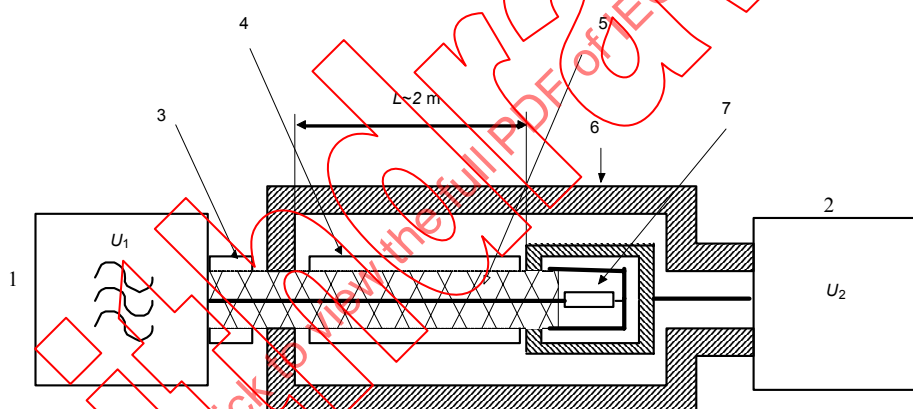
It suggests itself to limit the free space such that the said problems don't occur but wave propagation near the cable surface is not significantly changed. A triaxial measuring set-up is the solution. It has a one-sided short circuit between the metal tube and the cable screen. Power is fed into the terminated inner circuit of the cable and the disturbing power is measured at the opposite end of the outer circuit.

9.3 Theory of the triaxial measuring method

On the basis of the known reversibility of primary and secondary measuring circuits, the proposed measuring set-up, presented in Figure 45, is similar to the triaxial set-up for measuring the transfer impedance. The benefits of feeding the inner system, which is terminated by its characteristic impedance, are the matching of the generator and reflection free wave propagation over the cable length.

The characteristic impedance of the outer circuit depends on the diameter of the measuring tube and the cable design. The effect of the mismatch in the outer circuit is discussed later on.

The equivalent circuit using lumped circuit elements (shown in Figure 46) facilitates the understanding of the theoretical relationships.



Key

- | | |
|---|------------------------------------|
| 1 signal generator | 5 cable screen |
| 2 calibrated receiver or network analyzer | 6 tube |
| 3 input voltage to cable under test | 7 terminating resistor $R_1 = Z_1$ |
| 4 cable sheath | |

IEC 939/10

Figure 45 – Triaxial measuring set-up for screening attenuation

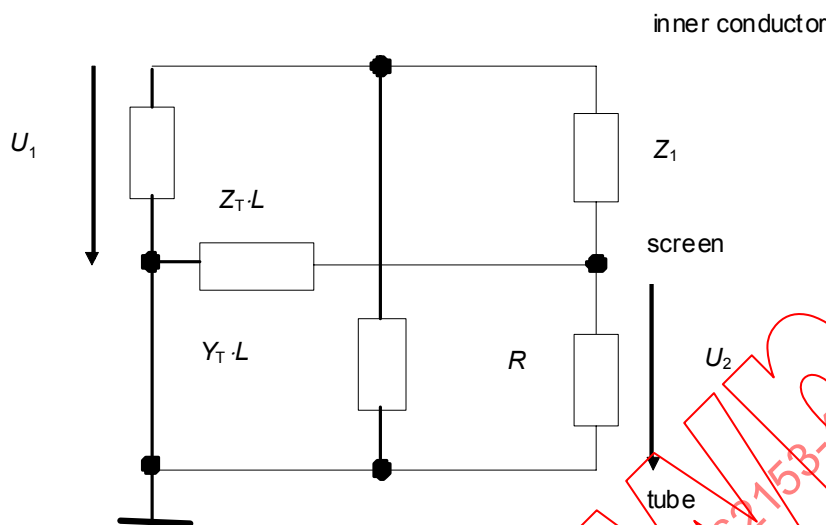


Figure 46 – Equivalent circuit of the triaxial measuring set-up

Based on the conditions of the objects to be measured it is assumed that the transfer impedance Z_T is low and the reciprocal quantity of the coupling admittance Y_T is high in comparison with the characteristic impedances Z_1 and Z_2 and the load resistance R . Therefore the feedback of the secondary circuit on primary circuit can be neglected.

When the frequency is low one may consider the primary circuit shown in Figure 46 as a voltage divider and read the disturbing voltage ratio directly. The one-sided short circuit in the measuring circuit prevents the efficiency of the capacitance coupling admittance Y_T .

$$\frac{U_2}{U_1} \approx \frac{Z_T \cdot L}{Z_1} \quad (38)$$

In the high frequency range, where wave propagation has to be considered, one may expect the transfer impedance to be proportional to the frequency in most cases. Therefore it is expedient to use the following equation:

$$Z_T = R_T + j \cdot \omega M_T \approx j \cdot \omega M_T \quad (39)$$

and consider the effective mutual inductance per unit length M_T at high frequencies as an approximated constant quantity as it is usually done with the through capacitance C_T .

It is common practice to describe the capacitive coupling in the form of the capacitive coupling impedance Z_F , which is nearly invariant with respect to the geometry of the outer circuit (tube). [24, 27]

$$Z_F = Z_1 Z_2 Y_T = Z_1 Z_2 \cdot j \cdot \omega C_T \quad (40)$$

Furthermore, the attenuation constants α_1 and α_2 of the circuits may generally be neglected as, for example, the value of nearly 1 dB/m of the common cable type RG 58 at 3 GHz is relatively small compared to the usual measuring uncertainty.

In the relevant literature it is common practice to describe wave propagation in the form of phase constant [24, 25]. If the ratio between effective length and wave length is used instead of

the phase constant, the periodic phenomena become clearer. With wave length λ_0 in free space or λ_1, λ_2 in the circuits 1 and 2, the following relation exists:

$$\beta_{1,2} \cdot L = 2\pi \cdot \sqrt{\varepsilon_{r1,2}} \cdot \frac{L}{\lambda_0} = 2\pi \frac{L}{\lambda_{1,2}} \quad (41)$$

According to the theory of wave propagation [25] and line crosstalk [26], a wave propagates in the matched inner circuit towards the matched end. In the outer circuit a part of the induced wave propagates forwards to the measuring receiver and the other part is moving backwards to the short circuit. The total reflection at the short circuit reverses this backward wave and superposes it to the original forward wave, i.e. the sum can be obtained as measured value.

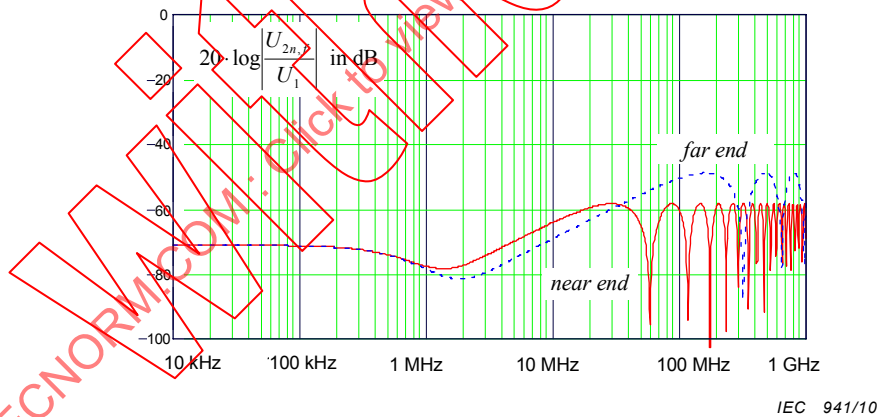
If the second circuit is matched at both ends the backward wave would be measured at the generator end (near end) and the forward wave at the opposite end (far end) separately.

Hence equations for the near end are derived from [24]

$$\frac{U_{2n}}{U_1} = \frac{Z_T + Z_F}{2Z_1} \frac{c_0}{j \cdot \omega (\sqrt{\varepsilon_{r1}} + \sqrt{\varepsilon_{r2}})} \left\{ 1 - e^{-j \cdot 2\pi (\sqrt{\varepsilon_{r1}} + \sqrt{\varepsilon_{r2}}) \frac{L}{\lambda_0}} \right\} \quad (42)$$

and for the far end

$$\frac{U_{2f}}{U_1} = \frac{Z_F - Z_T}{2Z_1} \frac{c_0}{j \cdot \omega (\sqrt{\varepsilon_{r1}} - \sqrt{\varepsilon_{r2}})} \left\{ 1 - e^{-j \cdot 2\pi (\sqrt{\varepsilon_{r1}} - \sqrt{\varepsilon_{r2}}) \frac{L}{\lambda_0}} \right\} \cdot e^{-j \cdot 2\pi \frac{L}{\lambda_2}} \quad (43)$$



Calculation parameters

C_T	=	0,02	pF/m	M_T	=	0,4	nH/m
R	=	50	Ω	L	=	2	m
Z_1	=	50	Ω	ε_{r1}	=	2,3	
Z_2	=	120	Ω	ε_{r2}	=	1,1	

Figure 47 – Calculated voltage ratio for a typical braided cable screen

With a short circuit and an unmatched measuring receiver these original voltage waves cause additional voltage portions. The sum of all voltage portions is zero at the shorted end (near end) and U_2 at the receiver end (far end). By use of the wave parameter and reflection factors or terminating resistors it is possible to calculate all voltage portions and the voltage U_2 from the primary induced voltage waves, Equations (42) and Equation (43) as follows:

$$\left| \frac{U_2}{U_1} \right| \approx \left| \frac{Z_T - Z_F}{\sqrt{\varepsilon_{r1}} - \sqrt{\varepsilon_{r2}}} \cdot [1 - e^{-j\varphi_1}] + \frac{Z_T + Z_F}{\sqrt{\varepsilon_{r1}} + \sqrt{\varepsilon_{r2}}} \cdot [1 - e^{-j\varphi_2}] \right| \cdot \left| \frac{1}{\omega Z_1} \right| \cdot \left| \frac{c_0}{2 + (Z_2/R - 1) \cdot (1 - e^{-j\varphi_3})} \right| \quad (44)$$

or in consideration of Equations (39) and Equation (40)

$$\left| \frac{U_2}{U_1} \right| \approx \left| \frac{M_T/Z_1 - C_T Z_2}{\sqrt{\varepsilon_{r1}} - \sqrt{\varepsilon_{r2}}} [1 - e^{-j\varphi_1}] + \frac{M_T/Z_1 + C_T Z_2}{\sqrt{\varepsilon_{r1}} + \sqrt{\varepsilon_{r2}}} [1 - e^{-j\varphi_2}] \right| \cdot \left| \frac{c_0}{2 + (Z_2/R - 1) \cdot (1 - e^{-j\varphi_3})} \right| \quad (45)$$

where

$$\varphi_1 = 2\pi (\sqrt{\varepsilon_{r1}} - \sqrt{\varepsilon_{r2}}) \frac{L}{\lambda_0} \quad \varphi_2 = 2\pi (\sqrt{\varepsilon_{r1}} + \sqrt{\varepsilon_{r2}}) \frac{L}{\lambda_0} \quad \varphi_3 = \varphi_2 - \varphi_1 = 4\pi \sqrt{\varepsilon_{r2}} \frac{L}{\lambda_0}$$

Calculated results for a typical braided cable screen are given in Figure 49. Another way to obtain the related induced voltage is given in [21].

The functional equation (Figure 48)

$$|1 - e^{-j\varphi}| = |2 \times \sin(\varphi/2)| \quad \text{with } \varphi = \varphi_1, \varphi_2, \varphi_3 \quad (46)$$

shows, that the equation of the voltage ratio contains three periodic partial functions of the ratio effective length L to wave length λ_0 :

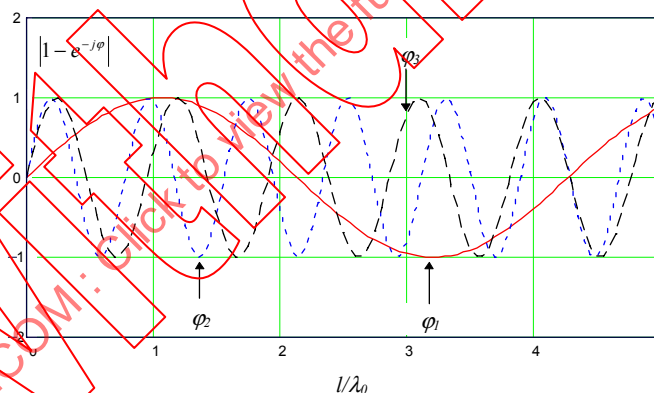
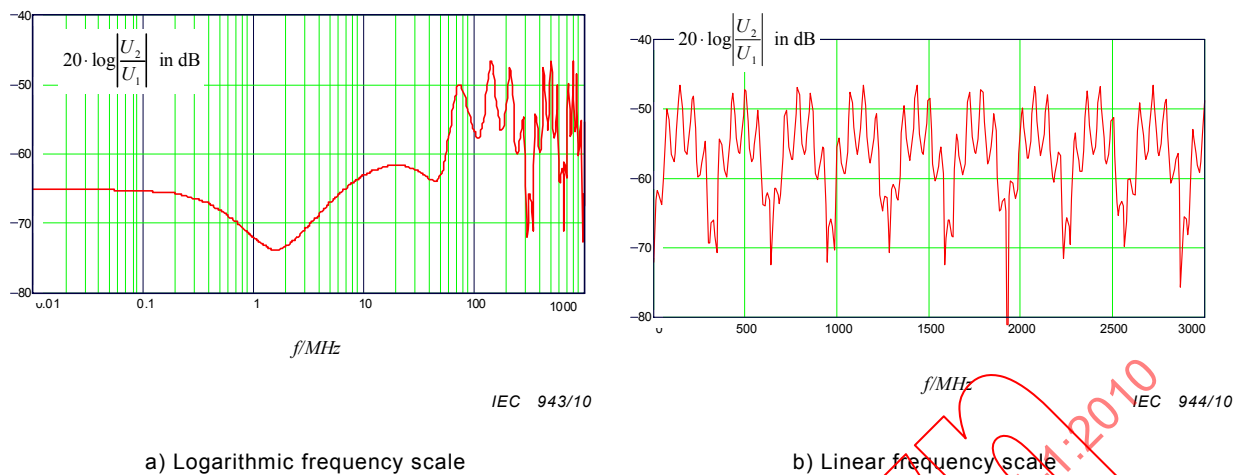


Figure 48 – Calculated periodic functions for $\varepsilon_{r1} = 2,3$ and $\varepsilon_{r2} = 1,1$

For low frequencies, when $L \ll \lambda_0$ and, consequently, $\sin(\varphi) \approx \varphi$, Equation (44) changes into Equation (38), the result of the common measuring method for the transfer impedance.

An example of the theoretical curve of the voltage ratio is shown in Figure 49 in two diagrams. The left one, a) with a logarithmic scale to extend the lower frequency range and the right one b) with a linear scale up to very high frequencies.



Calculation parameters

C_T	=	0,02	pF/m	M_T	=	0,4	nH/m
R	=	50	Ω	L	=	2	m
Z_1	=	50	Ω	ϵ_{r1}	=	2,3	
Z_2	=	120	Ω	ϵ_{r2}	=	1,1	

Figure 49 – Calculated voltage ratio-typical braided cable screen

It is not useful to specify the induced power for an exact length of cable at a single frequency, anywhere between a minimum and maximum of the function. Only the periodic maximum voltage is important for the evaluation of the screening effectiveness. In the outer circuit, the wave propagation shall be nearly the same as in free space. Therefore, the characteristic impedance Z_2 is higher than the common input resistance R of the measuring receiver, i.e. 50 Ω or sometimes 75 Ω .

Consequently, periodic maximum values of the voltage ratio are obtained from Equations (44) and Equation (45) which are independent of the input resistance of the receiver R and of effective cable length L .

$$\left| \frac{U_2}{U_1} \right|_{\max} \approx \frac{C_0}{\omega Z_1} \cdot \left| \frac{Z_T - Z_F}{\sqrt{\epsilon_{r1}} - \sqrt{\epsilon_{r2}}} + \frac{Z_T + Z_F}{\sqrt{\epsilon_{r1}} + \sqrt{\epsilon_{r2}}} \right| \quad (47)$$

or in consideration of Equation (39) and Equation (40)

$$\left| \frac{U_2}{U_1} \right|_{\max} \approx \left| \frac{M_T/Z_1 - C_T Z_2}{\sqrt{\epsilon_{r1}} - \sqrt{\epsilon_{r2}}} + \frac{M_T/Z_1 + C_T Z_2}{\sqrt{\epsilon_{r1}} + \sqrt{\epsilon_{r2}}} \right| \cdot c_0 \quad (48)$$

At first sight C_T , Z_2 , ϵ_{r2} and Z_F appear as random quantities, which depend on freely chosen dimensions of the measuring tube. In reality, however, the voltage ratio is independent of the characteristic impedance of the outer circuit since $C_T \cdot Z_2$ and Z_F are practically invariant with respect to the dimensions of the measuring tube [24, 27]. Furthermore, the influence of the cable sheath on the resulting relative permittivity ϵ_{r2} is negligible if the design of the measuring tube takes into account the requirement for a wave propagation which is approximately the same as in the free space, in consequence $\epsilon_{r2} \approx 1,0$.

The periodic maximum value is independent of the effective length L and frequency f or wave length λ . A measured frequency response would hint at a frequency related quantity rather than the pure mutual inductance M_T .

As it is seen from Figures 48 and Figure 49 the envelope rise is reached with the first maximum of the wide period at:

$$\lambda_0/L \leq 2 \cdot |\sqrt{\epsilon_{r1}} - \sqrt{\epsilon_{r2}}| \quad \text{or} \quad f > \frac{C_0}{2 \cdot L \cdot |\sqrt{\epsilon_{r1}} - \sqrt{\epsilon_{r2}}|} \quad (49)$$

In this frequency range Z_T can be calculated if Z_F is negligible:

$$|Z_T| \approx \frac{\omega \cdot Z_1 \cdot |\epsilon_{r1} - \epsilon_{r2}|}{2 \cdot c_0 \cdot \sqrt{\epsilon_{r1}}} \cdot \left| \frac{U_2}{U_1} \right|_{\max} \quad (50)$$

9.4 Screening attenuation

The screening attenuation is defined as the logarithmical ratio of the maximum power in the secondary (outer) circuit to the power propagating in the primary (inner) circuit.

$$a_s = -10 \times \log_{10} \left(\text{Env} \left| \frac{P_{r,\max}}{P_1} \right| \right) \quad (51)$$

The power coupled into the outer circuit depends on Z_2 although the peak voltage is independent of it. Thus a normalised value of the characteristic impedance of the outer circuit Z_s must be defined. It is common practice to define $Z_s = 150 \, \Omega$ [24].

In the standardised "absorbing clamp method" (see 12.4 of IEC 61196-1), the outer circuit is matched with Z_2 , and the radiated power is the sum of the near end and far end crosstalk. From the comparison of that measuring circuit with the measuring circuit of the triaxial method result the relation of the measured power to the radiated power.

The equivalent circuit for an electrical short part of the length ΔL and for a negligible capacitive coupling illustrates the circumstances in Figure 50.

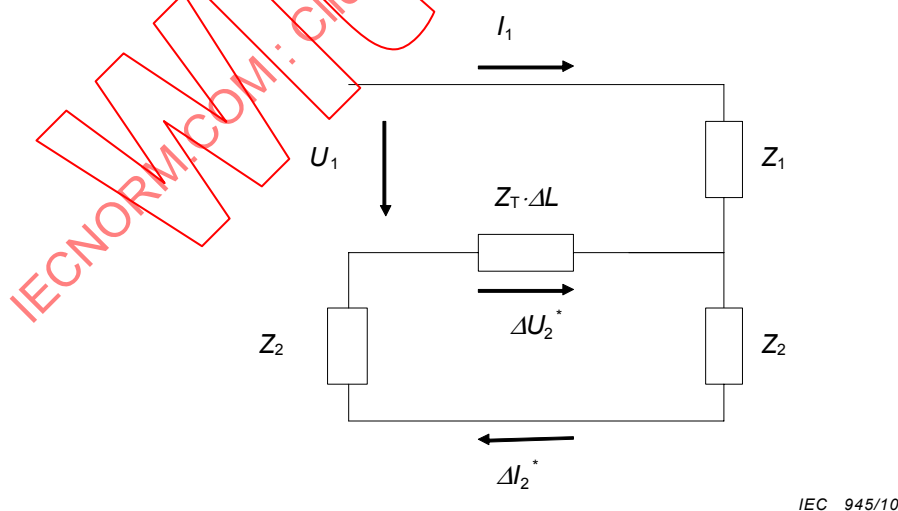


Figure 50 – Equivalent circuit for an electrical short part of the length ΔL and negligible capacitive coupling

The power in the primary circuit is: